

Image Based Techniques for Crack Detection, Classification and Quantification in Asphalt Pavement: A Review

H. Zakeri¹ · Fereidoon Moghadas Nejad¹ · Ahmad Fahimifar¹

Received: 30 July 2016 / Accepted: 29 August 2016 / Published online: 17 September 2016
© CIMNE, Barcelona, Spain 2016

Abstract Pavement condition information is a significant component in Pavement Management Systems. The labeling and quantification of the type, severity, and extent of surface cracking is a challenging area for weighing the asphalt pavements. This paper presents a widespread review on various platform and image processing approaches for asphalt surface interpretation. The main part of this study presents a comprehensive combination of the state of the art in image processing based on crack interpretation related to asphalt pavements. An attempt is made to study the existing methodologies from different points of views accompanied by extensive comparisons on three stages of methods—distress detection, classification, and quantification to facilitate further research studies. This paper presents a survey of the developed pavement inspection systems up to date. Additionally, emerging and evolution technologies considered to automate the processes are discussed.

1 Introduction

Visually inspecting the infrastructure and evaluating them by subjective human experts is the simplest method [277]. This approach, however, involves high labor costs and produces unreliable and varying results [87, 203]. Furthermore, it exposes the inspectors to dangerous working conditions on highways. Destructive Testing (DT) and Non-Destructive Testing (NDT) are both costly and time consuming [229, 288]. To overcome the limitations of the subjective visual evaluation process, various attempts have been made to develop semi-automatic and automatic procedures (Montero et al., [77, 114, 169, 191, 203, 285, 286]). Ideally, an automated system could be used as an alternative of the human eye, which could quickly detect and quantify diverse types of cracking and spalling in any size, in rapid collection speed, and different weather conditions [152, 226].

Recently, departments of road maintenance, repair and transportations have become more interested in using automatic systems for pavement assessment. The rate of making and utilization of computer vision methods for pavement engineering applications have been exponentially increased [114].

Recently, massive research attention has been given to developing automated and semi-automated procedures for pavement assessment and evaluation [114, 277]. Non-destructive evaluation techniques, such as Digital Image Processing (DIP) [77], Ground Penetration Radar (GPR) [213, 294], fiber optic sensors [34], laser systems (LS) or Hybrid systems (HS) [77, 213] are emerging procedures for health monitoring [30, 203]. For consistency and uniformity of data collection and promoting the data's quality, cost-effective automated systems and modified algorithms are proposed [2, 87, 277, 295, 296]. Most pavement

✉ Fereidoon Moghadas Nejad
moghadass@aut.ac.ir

H. Zakeri
h-zakeri@aut.ac.ir

Ahmad Fahimifar
fahim@aut.ac.ir

¹ Department of Civil and Environmental Engineering,
Amirkabir University of Technology, No. 424, Hafez Ave.,
Tehran, Iran

cracking analyzer systems use machine vision and image processing models to automate the process and moderate problems [2, 43, 229, 272]. However, due to the irregularities of pavement surfaces, there has been limited success in correctly detecting, classifying, and quantifying cracks. In addition, most systems require complex algorithms with high levels of computing power. While many attempts have been made to automatically collect pavement crack data, better approaches are necessary to evaluate these automated crack measurement systems under various conditions [48, 173, 229, 288, 295, 296]. Implementation costs, processing speed, repeatability, accuracy, objective and accurate detection or evaluation for these cracks and reducing the operation cost are very important tasks in this kind of system [77].

The characteristics of type, severity, and extent of pavement surface cracking are primary features for assessing the condition of asphalt pavements [246, 253]. For nearly all the methods, three groups have to be taken into account, the Image Acquisition Group (IAG), Image Processing Group (IPG) and Image Interpretation Group (IIG).

This paper covers these three groups and presents a survey of the developed semi-automatic and automatic systems for becoming up to date (Figs. 1, 2).

1.1 Image Acquisition Group (IAG)

Previously, Jahanshahi et al. [87], Koch et al. [114] and Chambon and Molirad [30] reviewed automatic distress detection methods and devices. Diverse types of systems have been used to simplify data gaining using equipped vans. Non-contact evaluation techniques classified as the Charge-Coupled Device (CCD) [165], Ground Penetration Radar (GPR), Laser Systems (LS) [109] or Hybrid systems (HS) [77, 149, 158] are innovative procedures for health monitoring [23, 30, 152].

Generally, these systems employ CCD cameras, thermal cameras, laser sensors, Electro-optical sensors [65], three-dimensional (3D) cameras [6, 149, 183] or a mélange of this device [61] like the Kinect sensor [158, 220].

Based on our knowledge, nearly all commercial systems need a powerful illumination system to prepare uniform

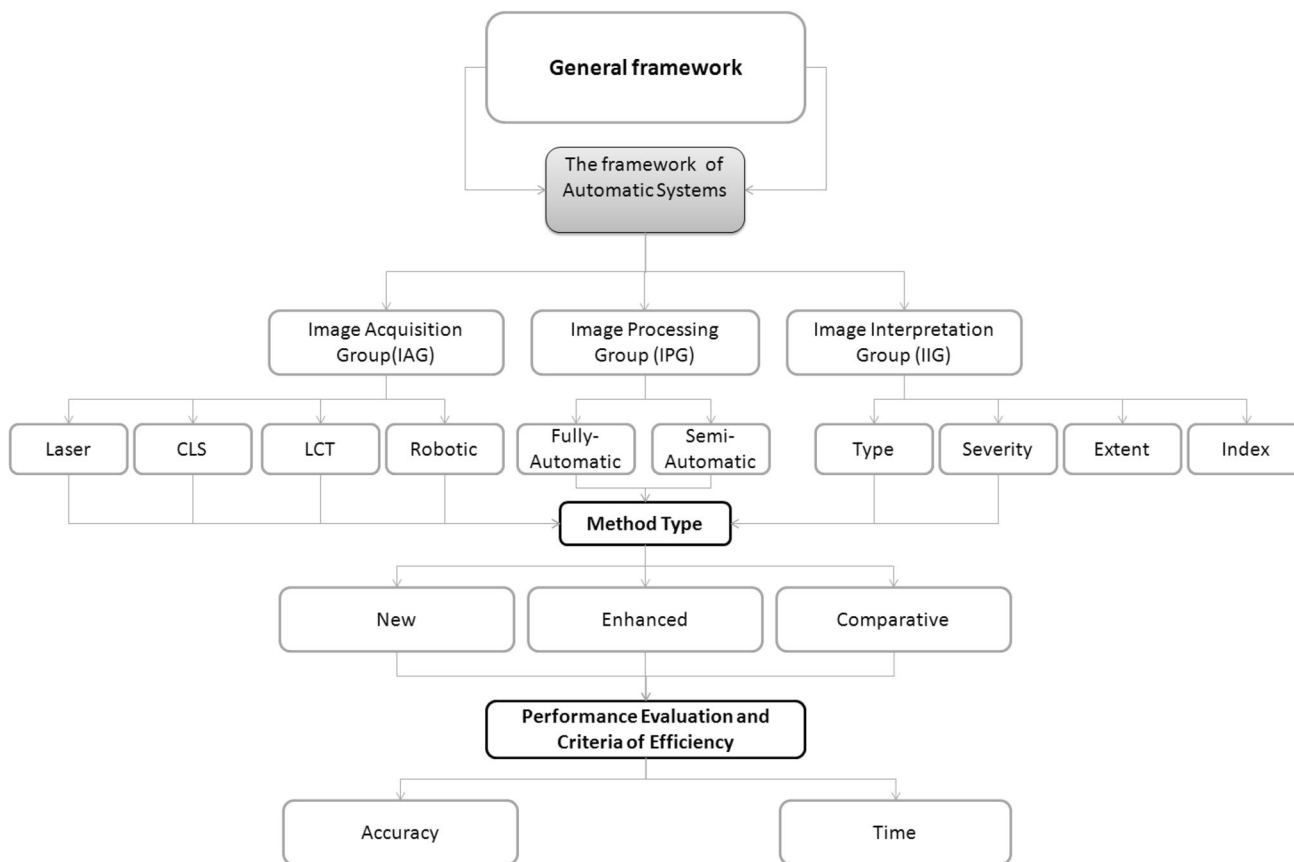


Fig. 1 The framework of automatic systems for pavement distress detection and classification

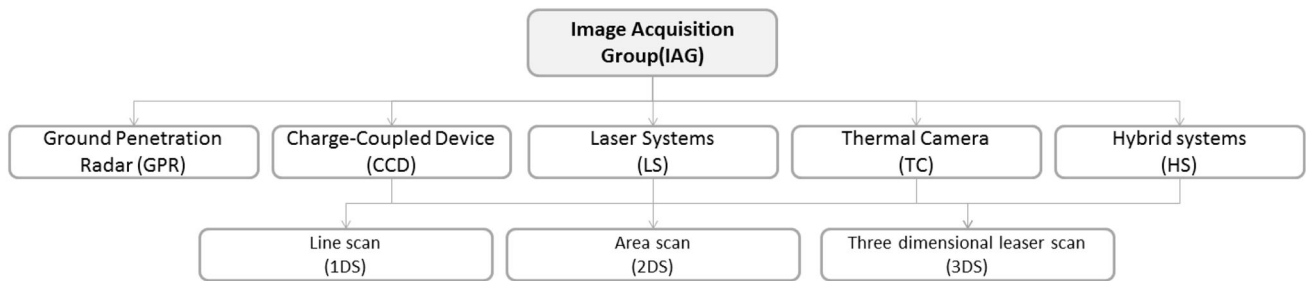


Fig. 2 The framework of IAS for pavement

lighting conditions for capturing images [218]. Automated Road Analyzer (ARAN), Digital Highway Data Vehicle (DHDV), Automated Distress Data Acquisition (ADDA), Automated Crack Monitor (ACM), SIRANO, Highways Agency Road Research Information System (HARRIS), Automated Distress Analyzer (ADA), AIGLE RN, AMAC, Profilograph and laser, Road Excellent Automatic Logging (REAL), Road Crack, ADVantage, PAVUE, CREHOS, RIEGL VMX-450 System [66], SIRANO and GIE are systems for capturing pavement surface images [30]. Manufacturing and supporting this equipment is very expensive and the result of the analysis highly depends on the circumstances and employed sensors [80, 153]. Additionally, images obtained from these systems are very discrete and automatically deciding on the type of distress is a difficult and time consuming task. Therefore, in order to improve the quality of images taken from the pavement, more powerful tools are needed.

Many scientists have developed inspection robots in order to increase safety and convenience during assessments [35, 40, 69, 211, 212]. Various motivations such as the safety, efficiency, and quality have promoted the increased use of robotic systems. The results demonstrate that the UAV is capable of carrying out difficult missions independently [185, 203]. The use of robotics rapidly increased in many fields of civil engineering because of its benefits [44, 100]. Some applications of robotics consists of: making highway material, construction of roads and pavement (including quality control and compaction), pavement maintenance and operations (including inspection and monitoring), and evaluation in unsafe and difficult-to-access locations like tunnels and bridges. However, it is luxurious and expensive. Robotics uses high technology and requires extraordinary facilities. It is sensitive, complicated, and often requires expensive machineries that need special training to operate and maintain.

The robotic systems [242] involve three parts according to Fig. 3: (1) A specially designed car, (2) A robot instrument and control system and (3) A machine vision system (Montero et al., [174, 235, 275, 297].

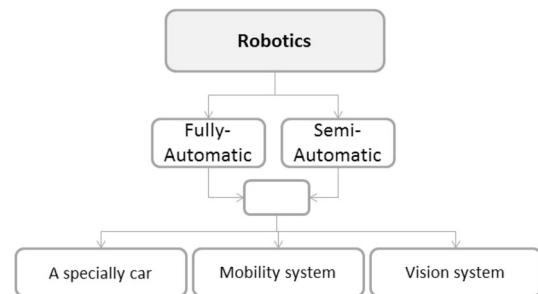


Fig. 3 The general components of robotic systems

Robots have superior flexibility, mobility and movement, are more appropriate and have the capability to moderate the labor required, making them very suitable for surveying responsibilities. Robots can operate without human control which means they are autonomous and independent. Robots can convey several kinds of devices and integrate with different controllers [235].

Recently, scientists have made wide applications in the field of the UAV system for the unmanned aerial vehicle (UAV) for the monitoring of structures and maintenance controls (1999, [19, 155, 185, 195, 280]. The potential of UAV is recognized by modern photogrammetry and remote sensing [46]. The UAV systems provide a new platform for data acquisition [195, 212]. They believed that the experiences with the UAV systems are useful and practical for other applications [19, 84, 212]. These systems are tested in autonomous surveillance, photogrammetric for 3D modeling, remote-sensing, monitoring of bridges and super structures, infrastructures like pipelines, bridges and roads [212]. Recently, Zhang and Elaksher presented a UAV based imaging system for the 3D evaluation of rural roads surface distresses [284]. It was good demonstrating the potential of this sort of system for future practice. This is mainly due to the low cost, fast speed, high maneuverability, and high safety of UAV systems for collecting images. UAVs are already replaced over satellites and manned vehicles. Moreover, they have overcome the disadvantage of low flexibility and high cost of aerial imagery [46]. Quadcopters have distinct advantages compared to other existing UAV approaches. Some of the advantages

are its low cost of manufacturing and maintenance, its flexibility and maneuverability to work in a very hard and complex surveying mission, the controllability in both autonomous and pilot mode, and manageable in abnormal circumstances, like storm, winds, snowy and rainy weather. In this paper, a new attempt has been made to use a Quadcopter UAV instrument to capture pavement images [284]. Table 1 shows a survey vehicle for the collection of data at normal speeds.

The new robotic developed is a Quadcopter Unmanned Aerial Vehicle (QUAV) for pavement inspection. The QUAV was selected because of its low cost and high flexibility to operate in a very complicated mission. The hardware architecture is shown in Fig. 4. The developed system—Rahbin—is assembled with:

Four sets Tarot 4114 320 kV Out runner Brushless Motor, 4 set 40 Amp OPTO Brushless Motor, ESC Speed Controller, Carbon Fiber Quad copter Frame, Main controller, Power Management Unit (PMU), GPS, LED, flight control, telemetry system, GoPro 2Axis Brushless Gimbal All Multi-Rotor, Head Track Video Goggles and LCD for monitoring, 5.8 GHz 8CH FPV Transmitter for sending data, AV Receiver, LCD, and 2 set Radio controller.

Its total size in diameters is 100 cm. The QUAV is able to produce an absolute thrust of 3 kg. Its empty (without battery and camera) and gross weight is 500 and 1000 g, respectively. The flight control system serves both aided and programmed mode. An autopilot software (Grand Station NAZA-M V2) is utilized on the main computer system. The software GUI enables the user to define a mission plan according to Google map and sets the height, speed, rote mission, and resolution of distress. Additionally, 3D MapDisplay, Real-time Flight Monitoring, One Key Takeoff, Joystick/Keyboard Mode, One Key Go Home, Click Go Mode, Waypoints Editing, Automatic Takeoff and Landing, F Channel Controller, General Purpose Servo Action and Photogrammetric Tool can be used. The Gopro Camera has a wide range of resolution (5, 7, 12, 14 Mega pixel). The Flight Control Unit (FCU) is the central part of the QUAV. It is able to apply autonomous inspection based on predefined scenarios. The Inertial Measurement Unit (IMU) is used to identify the additional information data (such as alignment, acceleration, and altitude). The four Brushless set motor controllers receive their orders from the FCU to adjust the rotational speed of the motors. The FCU is connected to a GPS receiver and a compass to increase navigational capabilities.

Since it is very maneuverable—‘location hold’, ‘coming start point’, and ‘flight according to pre identified waypoints’—it could be useful in all kinds of situations and dangerous positions for surveillance. An expert can generate the new waypoints based on the footprint of regions of interest, for example flying the QUAV in a circle,

network, polyhedral, zigzag, curved or other more complex patterns with the ability of staying in the air for 45 min and a distance of nearly 7 km at the speed of 4 m/s. The QUAV used in this work required it to travel above 2000 m with a variable operating altitude in the range of [1–100] m. However, it is not restricted. The pavement surface information of the lane is collected via a transmitter device sent to the host computer, where the proposed method for classification of pavement distress algorithms is implemented. The images that show distress will be detected and saved in the pavement Distress Data Base (DDB). Also, the positioning information indicating where the images are taken that is obtained from a global positing system is saved. Existing systems have shown good performance to collect new forms of pavement surface images.

From Table 1 it can be extracted that the current state-of-the-art Image Acquisition Group (IAG) works well with the mechanization of data collecting. However, there are currently no intelligent platforms available that work autonomously, with low cost and high speed. With the growth of technology, the number of automatic and robotic systems grows quickly. The USA is the greatest user of the system. However, other countries are interested in using this technology seriously. More than any sensor, the two-dimensional (2D) camera is used. Recently, the Robotic Image Acquisition (RIA) system, as an emerging technology over other systems, has been addressed for management and inspection. Smart flying robots will be replaced by experts and automatic/semi-automatic systems in the coming years.

1.2 Image Processing Group (IPG)

Recently, pavement surface image processing played a central role in automatic bridges and pavement assessment systems and scientists have paid more attention to this field [160], 1994, [30, 87]. Champion and Moliard [30] mentioned that image processing is an important step for the success of the automatic road pavement assessment [30]. Based on a review about image processing methods for pavement crack detection and classification, every method can be exploited in six assumptions [30]:

Based on Table 2, assumptions H_{G3} , H_{PGH1} and H_{T1} have a small degree of ambiguity that is also ambiguous. The use of fuzzy theory, especially the Type II, can lead to good results (Figs. 5, 6, 7).

The Histogram Analysis Methods are widely used methods. These methods are fast and simple in the field of image processing. However, the mathematical morphological tools show better results than HAM's. The next group is learning tools that are not fast and fully automatic methods. The Filter based method is not fully adoptive because the scale, size and width of cracks is not constant

Table 1 The semi-automatic and automatic image acquisition systems based on different IAG, dimension and method type

| No. | References | Year | Country | IAG | Dimension | Method | Speed (Km/h) | Use |
|--|---|-------------------------|-----------|-----|---------------------------|--------|--------------|---------|
| 1 | ADDA Jahanshahi et al. [86] | 1991 | USA | CCD | 2DS | SAI | M | P-APR |
| 2 | ACM Chambon and Moliard [30] | 1991 | USA | CCD | 2DS | SAI | M | P-APR |
| 3 | SIRANO Chambon and Moliard [30], Jahanshahi et al. [86] | 1991 | France | CCD | 2DS | SAI | M | P-APR |
| 4 | HARRIS Pynn et al. [187] | 1999 | UK | LS | 1DS + 3DS | AIA | H | N-APR |
| 5 | ADA-APSI-4096 Chambon and Moliard [30] | 2007 | USA | HS | 3DS + 2DS | SAI | H (100) | P-APR |
| 6 | AIGLE RN Chambon and Moliard [30] | 2008 | France | CCD | 2DS | SAI | M | P-APR |
| 7 | AMAC Chambon and Moliard [30], Jahanshahi et al. [86] | 2004 | France | HS | 1DS + 2DS + 3DS | SAI | H | N-P-APR |
| 8 | Profilograph and laser Chambon and Moliard [30] | 2007 | Denmark | LS | 3DS | SAI | H | N-APR |
| 9 | REAL Chambon and Moliard [30] | 1992 | Japan | HS | 3DS + 2DS | AIA | H | N-P-APR |
| 10 | ARAN Jahanshahi et al. [86] | 2003 | Canada | HS | 3DS + 2DS | AIA | H | N-P-APR |
| 11 | PAVUE | 1999 | Sweden | CCD | 2DS | AIA | H | P-APR |
| 12 | RPDIS Ferguson et al. [56] | 2003 | Australia | CCD | 2DS | AIA | H | N-APR |
| 13 | ASDMS | 2005 | USA | CCD | 1DS | LS | H | P-APR |
| 14 | VSdT Laurent and Doucet [121] | 2005 | Canada | LS | 1DS | AIA | H | P-APR |
| 15 | RoadCrack Chambon and Moliard [30] | 1999 | Australia | CCD | 2DS | AIA | H (105) | P-APR |
| 16 | PCDS 长安大学 [300] | 2009 | China | LS | 1DS | AIA | H | P-APR |
| 17 | HSPSSPS Reeves [194] | 2011 | Australia | CCD | 2DS | L | H | L-APR |
| 18 | APIS | 2011 | Iran | CCD | 2DS | L | M | L-AIA |
| 19 | APCA Jahanshahi et al. [86] | 2013 | USA | HS | 3DS | SAI | M | L-P-APR |
| 20 | RIEGL VMX-450 Guan et al. [66] | 2015 | China | HS | 3DS + 2DS | AIA | H | P-APR |
| 21 | Tadbir gar | 2008 | Iran | HS | 3DS + 2DS | SAI | M | P-N-APR |
| 22 | Bostan sanaat | 2013 | Iran | CCD | 2DS | SAI | H | N-APR |
| 23 | ACSM Kim et al. [110, 112] | 1998 | USA | CCD | 2DS | RIA | S | P-APR |
| 24 | LCSM and 2TLS Velinsky et al. [240], Yoo and Kim [273] | 1998 | USA | CCD | 2DS | RIA | S | P-APR |
| 25 | OCCSM Velinsky et al. [240] | 2003 | USA | CCD | 2DS | RIA | S | P-APR |
| 26 | ARMM Kim et al. [110, 112], Kim and Haas [111] | 1997 | Korea | CCD | 2DS | RIA | S (1.08) | P-APR |
| 27 | ACSTM Yoo and Kim [273] | 2015 | Korea | CCD | 2DS | RIA | S | P-APR |
| 28 | PathRunner | 1990 | USA | HS | 3DS | AIA | H | N-APR |
| 30 | Samsung | | USA | CCD | 2DS | RIA | S | P-APR |
| 31 | An innovative UAV Zhang and Elaksher [284] | 2012 | USA | HS | 3DS | RIA | H | P-UPR |
| 32 | UAV Grandsaert [64] | 2015 | USA | HS | 2DS | RIA | H | L-APR |
| 34 | Rahbin: QUAV | 2016 | Iran | CCD | 2DS | RIA | H | L-P-APR |
| Image acquisition group (IAG) | | Dimension | | | Use | | Speed | |
| Ground penetration radar (GPR) | | Line scan (1DS) | | | Laboratory (L) | | Low (L) | |
| Charge-coupled/digital device (CCD) | | Area scan (2DS) | | | Project (P) | | Medium (M) | |
| Laser systems (LS) | | Three dimensional (3DS) | | | Network (N) | | High (H) | |
| Hybrid systems (HS) | | | | | Concrete paved road (CPR) | | | |
| Method | | | | | Asphalt paved road (APR) | | | |
| Semi-automatic image acquisition (SAI) | | | | | Unpaved road (UPR) | | | |
| Automatic image acquisition (AIA) | | | | | | | | |

Table 1 continued

| Image acquisition group (IAG) | Dimension | Use | Speed |
|---------------------------------|-----------|-----|-------|
| Robotic image acquisition (RIA) | | | |

ADDA automated distress data acquisition, *HARRIS* highways agency road research information system, *ACM* automated crack monitor, *APCA* autonomous pavement condition assessment (University Of Southern California), *SPS* stereo pavement scanner, *RPDIS* road pavement deterioration inspection system, *ASDMS* automated surface distress measurement system (The University Of Texas System), *VSDT* vision system and a method for scanning a traveling surface to detect surface defects thereof (Institute National D'optique), *PCDS* pavement crack detection system based on image and the detection method thereof, *ADA* automated distress analyzer, *DHDV* digital highway data vehicle, *APSI-4096* automated pavement surface imaging model 4096, *REAL* road excellent automatic logging system, *HSPSSPS* high speed photometric stereo pavement scanner, *ARMM* automated road maintenance machine, *OCCSM* operator controlled crack sealing machine, *TTLS* transfer tank longitudinal crack sealer, *APCS* automated pavement crack sealer, *APIS* automated pavement inspection system, *ACSTM* automated crack sealer with telescopic manipulator, *ARMM* automated road maintenance machine, *ACSS* automated crack-sealing machine, *LCSM* longitudinal crack sealing machine, *2TLS* transfer tank longitudinal sealer

[126, 208, 232]. Most approaches in the model based methods are based on local/global analysis [30, 80, 114, 173, 226, 229, 246, 247, 279, 288, 295, 296, 298].

1.2.1 Pre-processing (PPS)

The asphalt pavement images are not captured under the same lighting condition (day/night), (sun/cloud) and some of them contain unwanted objects like random particle textures, inhomogeneity [263], non-uniform illumination and irregularities in the surface of the pavement, [289] shadows [282], very noisy environment lines [4, 175], water, tire marks, oil spills [219] and etc. As a result, selecting a uniform threshold is a very challenging issue in the segmentation step, therefore designing an effective pre-processing step is vital for obtaining good results [114, 159, 167, 168]. This step is related to accentuation, or sharpening features like edges, boundaries, or contrast to analysis. Image enhancement covers a wide range of classes including noise reduction, fuzzy edge eliminating, filtering, interpolation, magnification, contrast stretching, histogram modeling, transform operations, false coloring and pseudo coloring. The challenging part of pre-processing is quantifying for enhancement. Nearly all of these approaches are empirical and require an interactive procedure to get the optimum results. In the field of pavement distress analysis, some of the common image enhancement techniques are shown in Fig. 8.

Point operations are zero memory which are mapped into gray level based on transform $v = f(u)$. Contrast stretching, noise clipping and thresholding, gray-level windows slicing, bit extraction, bit removal and range compression are several of these transformations.

Many methods are based on spatial operations performed on local neighborhoods of input pixels. These kinds of enhancement operators convolved with an image called spatial mask. The spatial averaging and low pass filtering, directional smoothing, median filtering, un-sharp mask and crisper, spatial low pass, high-pass, and band-pass

Fig. 4 The general components of **a** semi-automatic (SAI) and automatic image acquisition (AIA), **b** kinect sensor [85, 158], **c** RIEGL VMX-450 a system with an inset picture of the laser scanners, cameras, and the navigation system [66, 265], **d** Telemaster UAV [64] and **e** Robotic Image Acquisition (RIA) systems

filtering, inverse contrast ratio mapping and statistical scaling, magnification and interpolation are some examples of this operator.

The next class is the transform operation enhancement method in which zero-memory operators are performed on a transformed image followed by the inverse transformation. Generalized linear filtering, root filtering, generalized spectrum, and homomorphic filtering are several examples of this operator.

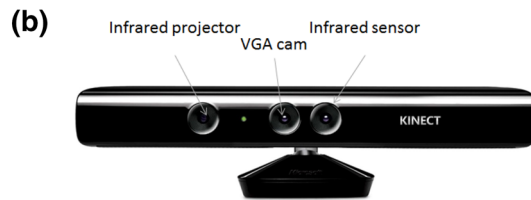
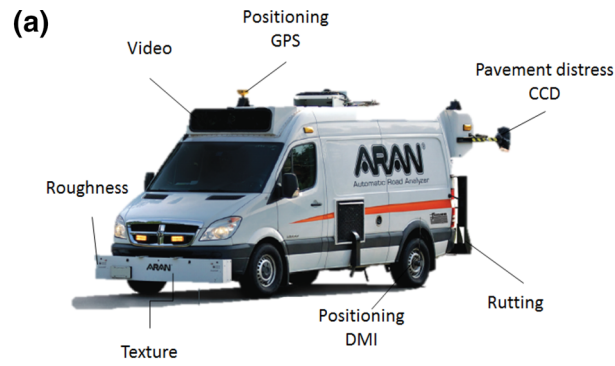
Generally, these methods are application dependent, and the final enhancement algorithm can be obtained by trial and error. Modern approaches employ hybrid or complex functions, which enable the user to enhance the image based on its applications (detection, classification, and quantification).

Yao et al. [267] have developed a new imaging system with the ability of scan pavement surface without using any artificial lighting for solving the noise and artifacts in images. The paired images [130] contain balancing details that are employed for making an image in which the shadows effects are moderated [267].

Gavilán et al. [61] proposed an adaptive road crack detection system by pavement classification. The first step was pre-processing that was carried out to both smooth the texture—spatial operation class—and enhance the linear features [61].

Zhou et al. [293] proposed an illumination invariant image enhancement and segmentation mode, which are crucial for feature extraction and classification. The experimental results show that the method was efficient for the illumination invariant and the irregularities in the surface of asphalt pavement [293].

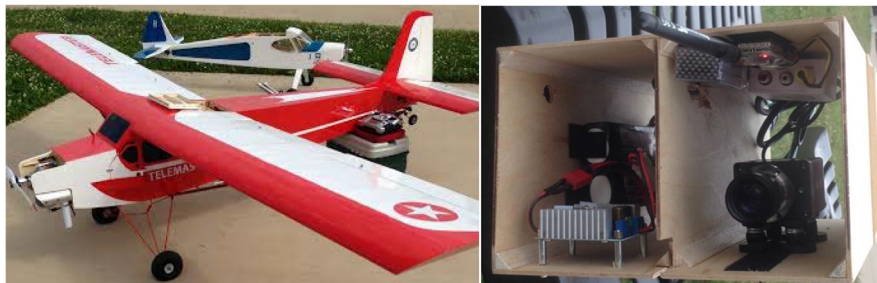
Jiang et al. [93] used a new crack enhancement algorithm based on the Electromagnetism-like Mechanism



(c) 1-Digital Camera 2-GNSS Antenna 3-Laser Scanners



(d)



(e)



Table 2 Various Assumptions based on semi-automatic and automatic crack analysis methods

| Assumptions | Description | References |
|-------------------|--|---|
| H _{P1} | Crack pixels are darker than the background | Chambon and Moliard [30], Amhaz et al. [7] |
| H _{P2} | Independence in the gray—level distribution | Zou et al. [298], Grandsaert [64] |
| H _{G1} | Thin continuous object | Oliveira and Correia [179], Tang and Gu [224] |
| H _{G2} | A set of connected objects | Jahanshahi and Masri [90], Tsai et al. [230] |
| H _{G3} | Various widths | Oliveira and Correia [179] |
| H _{PGH1} | Vague character of the points inside the crack | Tang and Gu [224] |
| H _{T1} | Pattern analysis in transformed domain | Salman et al. [202] |

Fig. 5 The general classification of hypotheses of Semi-automatic (SAI) and Automatic image processing (AIP) methods based on visual analysis

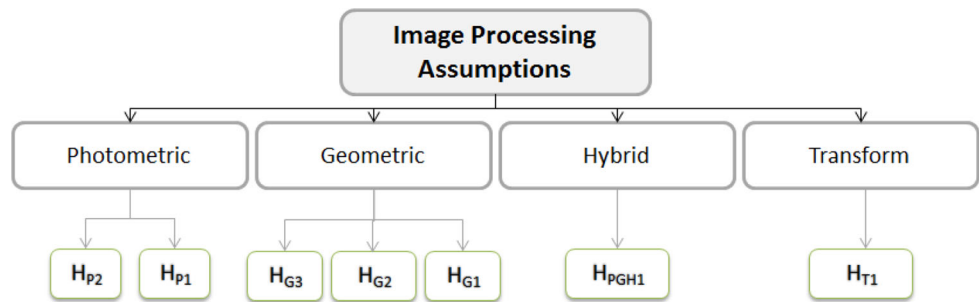


Fig. 6 Five families that are proposed for semi-automatic and automatic methods in the field of image processing distress detection and classification [30]

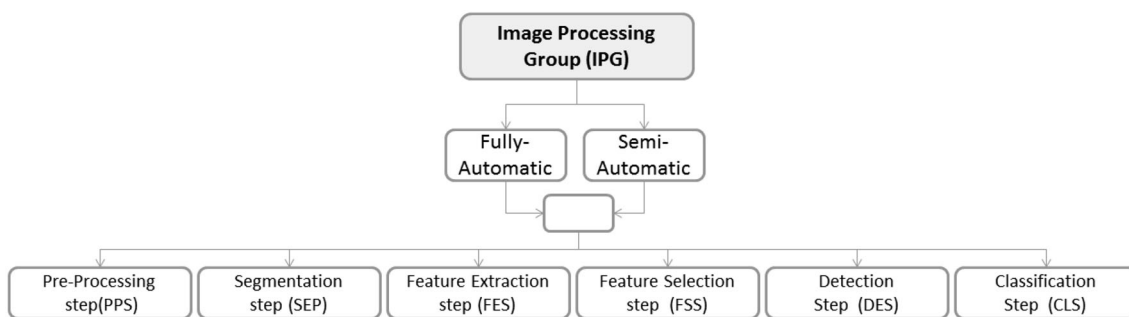
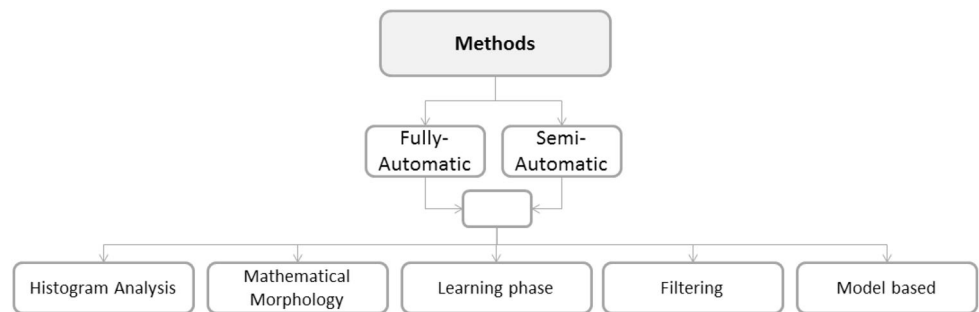


Fig. 7 The framework of IPG for pavement distress detection and classification

(EM) to interpret the crack images. Local neighborhoods of pixels are divided into strong and weak neighborhoods and noise points. The idea of Shuffled Frog-Leaping Algorithm (SFLA) is used in the EM Algorithm for linking global and local information search. Experimental consequences demonstrated that the algorithm proposed is good at crack

enhancement and it shows better performance in image segmentation [93].

Li et al. [130] used the grey entropy to the road surface image enhancement to lay a good foundation for the automatic detection of cracks. They applied the grey entropy to characterize the scale of the increase or decrease

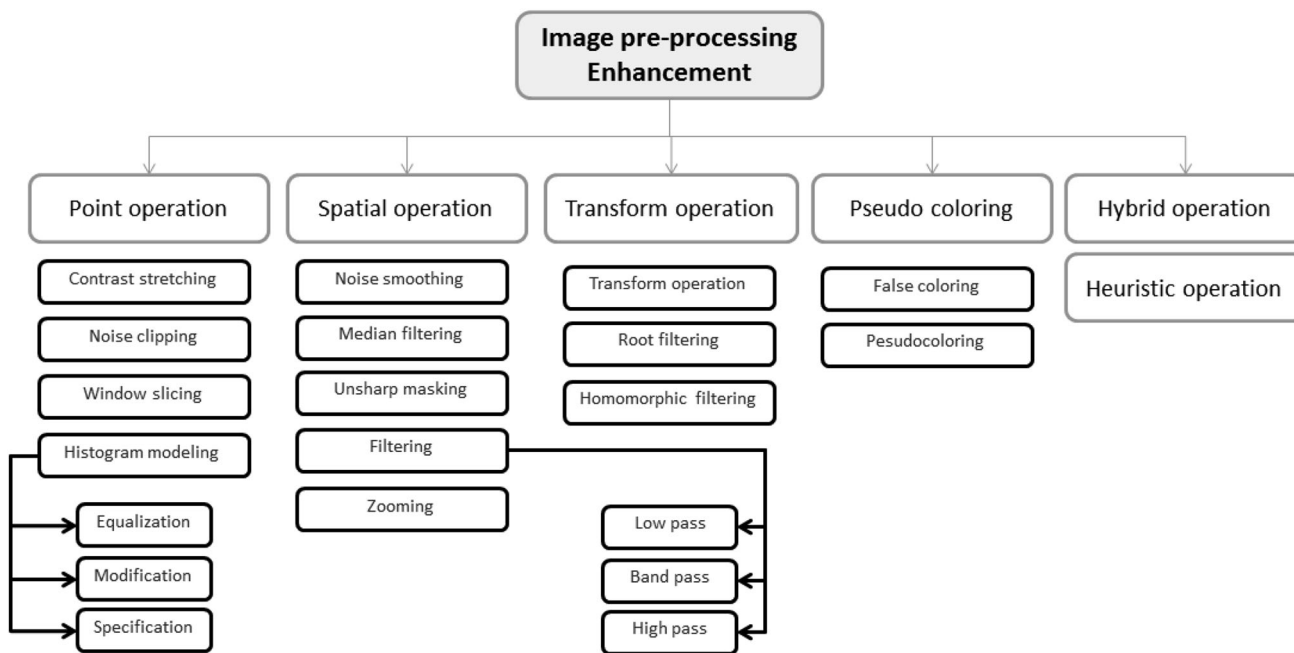


Fig. 8 The framework of common images enhancement methodologies

in the process of image local contrast enhancement. As a final point, simulation results demonstrated that the proposed method is more effective than other traditional algorithms.

Adu-Gyamfi et al. [3] used a multi-resolution image enhancement method based on Gaussian pyramids.

1.2.2 Segmentation (SEP)

Image segmentation is a process to extract the region of interest from the image [216]. It is vital for successful classification of pavement cracks [14]. It is an important step in image processing since it conditions the quality of the resulting interpretation [205, 206, 287]. It is important to extract the objects like crack and pothole. Several image segmentation methods have been proposed by scientists [91], and these techniques are classified in Fig. 9. The latest study on image segmentation methods is shown in Fig. 9 which is discussed in the field of pavement distress analysis.

Kan and Ravi [106] conducted a research on Image Segmentation Techniques, and classified segmentation into different groups: Threshold Based, Region Based, Edge Based, Fuzzy Theory Based, ANN Based and PDE (Partial Differential Equations) Based. They concluded that a hybrid method for image segmentation involving two or more methods is the best tactic for analyzing the image segmentation [106].

Basavaprasad and Ravi [15] have introduced a framework for a systematic comparative study on segmentation

based on Pixel based, Threshold based, Edge based and Region based segmentation. They conclude that there is no general segmentation technique that can be implemented for all kinds of images. On the other hand, a number of techniques shows better performance by a combination of suitable techniques [15]. The prior knowledge about images enable the user to adopt and select a better method to segment the image [15, 106].

In this section, we summarize a brief review of methods proposed in the literature based on the Fig. 9 classification in the field of pavement distress detection and classification, and then a new method based on hybrid theory will be proposed.

The overall analysis and discussion about segmentation of the surveyed methods will be presented in the current section. In this paper, the entire available segmentation methods new or developed and enhanced for pavement image analysis were discussed and their advantages were investigated. To present a comprehensive viewpoint to the readers for finding essential information about each technique, we have classified the entire methods in six classes. These six categories consist of: Edge based segmentation (EBS); Threshold based segmentation (TBS); Region based segmentation (RBS); Clustering based segmentation (CBS); Matching based segmentation (MBS); and Fuzzy Based Image Segmentation (FBS). Table 2 contains the collected information on the studied methods.

It can be observed that most of the approaches developed for segmentation try to use the Threshold based segmentation (TBS). These methodologies mostly develop

on basic principles of single thresholding. Based on this theory, the entire image pixel intensity value is compared with the selected threshold value. If a pixel value is larger than the threshold value, then those pixels are considered. Thresholding consists of: Global Thresholding and Local Thresholding and each one can be classified into: Simple/Single Thresholding, Multiple Thresholding and Optimal Thresholding [216]. In all methods, thresholding plays an important role in distress detection and classification.

On the other hand, similar methods on segmentation such as Clustering based segmentation (CBS); Matching based segmentation (MBS); and Fuzzy Based Image Segmentation (FBS) are rather scarce. This may be based on the low speed of these approaches. We can see that two major segmentation methods can be found in the literature. From these six categories, two papers present new segmentation methods while the remainder just apply them in pavement cracking cases. Therefore, segmentation has not received much research attention and except one new approach, no new effort has been made on uncertainty bounds of edge and branches of cracking in recent years [298].

Tasi et al. [233] compared six segmentation techniques, regression thresholding, edge detection (Canny), crack seed verification, wavelets, iterative clipping technique, and dynamic optimization-based thresholding to quantitatively evaluate the performance of various image segmentation approaches. Based on the test results, it was determined that the dynamic optimization-based technique shows better performance than the other methods for all of the images [233].

In contrast to Edge based segmentation (EBS), Threshold based segmentation (TBS) methods are increasing more and more. From 2004, when Zhou presented the first thresholding algorithm based on *Wavelet and Radon Transforms*, most multiresolution based approaches were concentrated on *time–frequency* [159, 167, 168] and other representation methods such as edge based Clustering based segmentation (CBS) and Matching based segmentation (MBS) seem to be less attractive to researchers [295, 296]. From the contents of Table 2, it can be concluded that higher simple methods are more practical in pavement distress segmentation.

Ayenu-Prah and Attoh-Okine [14] used bi-dimensional empirical mode decomposition (BEMD) for pavement crack evaluation. The proposed method explores pavement crack detection using BEMD together with the Sobel edge detector. The results are compared with results from the Canny edge detector.

Salari et al. [201] proposed an adaptive approach for pavement distress segmentation based on Genetic Algorithms. An objective function is used to maximize by applying the information theory to select the ideal threshold for segmentation [201].

Salari and Bao [199] use a novel color segmentation method based on a feed forward neural network to separate the road surface from the background. They also use a thresholding approach based on probabilistic relaxation to separate cracking from the pavement surface [199].

Huang and Tasi [79] proposed a fast algorithm based on dynamic programming-based (DP-based) for pavement crack segmentation. The proposed method incorporated the DP and grid cell. Based on this hybrid method, the region-based non-uniform background illumination was removed, and the pre-processed image was divided into grid cells. Experimental results showed that the hybrid method worked three times faster than the single DP-based approach [79].

Genetic programming has been used by Nishikawa et al. [173] for segmentation of distress, removing residual noise, and filtering the subjects in the backgrounds of the cracks to improve the results.

Texture-based features have been used to identify cracks from the asphalt pavement [237]. They used a group of regions pixels of coherent texture by over segmenting the image. The superpixels obtained are then classified by Multiple Instance Learning as either cracked or not cracked [237].

Lokeshwor et al. [141] presented a robust technique for automated segmentation of cracks from the road surface based on imaging systems under natural lighting based on the adaptive thresholding technique and user defined decision logic. To evaluate the performance, three fast image segmentation algorithms—Canny edge detection, iterative clipping and weighted mean based adaptive thresholding—are assessed based on noisy road surface

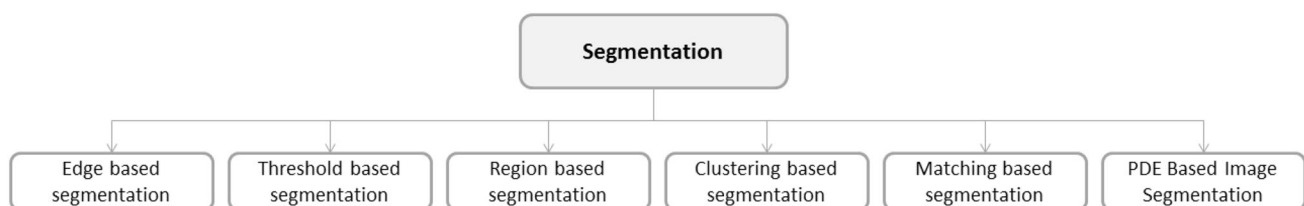


Fig. 9 Image segmentation methods

images. Based on this research, the weighted mean based adaptive thresholding technique shows better performance. The experimental results demonstrated that this method works with accuracy up to 96 % [141].

Guan et al. [67] have proposed the ITV Crack method for segmentation, an ITV-based framework for extracting cracks in road surfaces from MLS point clouds. The ITV Crack worked based on curb based road extraction, GRF image generation and ITV based crack extraction. They believed that one of the limitations is the intensive computation required due to the iterative operations involved in the tensor voting process. Using a multithread scheme, computational performance and time complexity will be greatly reduced [67].

Xu et al. [264] proposed the saliency concept into the challenging work of automatic pavement crack detection. Their method combines and improves the rarity and contrast based saliency measure. The proposed statistical feature extraction and Bayesian estimation method have greatly enhanced the saliency map. This suggests that spatial cracks shall be measured through the feature extraction. The experimental results demonstrated that this method has significantly outperformed several traditional EBS, TBS, PDE and MBS methods [264].

From Table 3 and Fig. 10 it can be concluded that MBS and TBS methods are used more than the others. It also means that FBS and PDE are less discussed. Based on the vague and fuzzy nature of the crack, as mentioned in Sect. 1–2, the FBS method is considered a good research area for future works.

1.2.3 Feature Extraction (FES)

The final purpose in pavement image processing like the other applications is to extract significant features, from which understanding and interpretation of the scene can be provided by the computer [92]. In image analysis, the input image is first preprocessed and then certain features are extracted for segmentation and classification. The segmented image is fed into the understanding system or segmentation system. Image classification draws diverse parts into one or several objects. For instance, in distress classification, all cracks identified as line shapes with branches may be classified as Multiple Crack (MC) and those without branches, as Single Crack (SC). A classification of feature selection methods is shown in Fig. 10.

The spatial feature (SFE) is characterized by its gray levels, their joint probability distribution, and spatial distribution [92]. For example, in pavement images, the amplitude of Radon transform represents the crack, which determines the size and severity of the crack being imaged [159, 167, 168, 295, 296]. Histogram feature extraction (HFE) is based on the histogram of the cracked section. Some of the prevalent histogram features are moments, absolute

moments, central moments, absolute central moments, entropy, mean, variance, average energy, skewness, kurtosis, median and modes. The frequency domain contains a useful hidden information in the data that can be extracted by Transform Features (TFE). Generally, the high transform feature, like High amplitude wavelet coefficient (HAWC), High Frequency Energy Percentage (HFEP) and STD in the frequency domain [295, 296] can be used for crack detection and the low frequency can be employed for surface analysis (skid resistance). Also, high pass filter, low pass filter, and bandlimited can be used for decreasing the periodic effect of texture. Different filters in frequency, like Discrete Fourier Transform (DFT), Harr, Hadamard, Daubechies, Coiflet, Sine, cosine, Slant, KLT, Radon Transform, Garbor Filter [279] Beamlet Transform [95, 137, 256, 271], Ridgelet Transform [136, 285, 286], Curvelet Transform [169], contourlet transform [143, 292], Shearlet Transform [258] are also useful for feature extraction [159, 167–169] (Fig. 11).

In the area of transportation infrastructure, image analysis, and specially edge detection (EFE) is a challenging issue. The edge detection method is not an easy task to select or be used because of complexity, diversity of pavement images and pavement distress's weak information [33]. Edge detection is an alternative method in the process crack detection and classification [247]. A wide range of edge detector methods are recommended in image processing. Based on the concept of gradient theory, one edge detection approach is to measure the gradient ∇ along radius ρ in direction θ , and five classes of edge detection have been proposed: (1) gradient operators (GO), (2) compass operators (CO), (3) Laplace operators (LO), (4) Zero crossing (ZC) and (5) Stochastic gradient (SG).

The first group works by a pair of mask which measures the ∇ in two orthogonal directions. Several common GO presented in some references are Fast Haar transform (FHT), Fast Fourier Transform, Sobel, and Canny [27], [145], Roberts, Laplacian of Gaussian (Log), Zerocross.

Some classical approaches like Sobel, Prewitt, and Kirsch are simple to detect edges, and their orientations are also fast and easy to operate. However, these procedures are sensitive to noise and are inaccurate. Zero Crossing based on Laplacian and second directional derivative, are responding to some of the existing cracks, and show sensitivity to noise. Laplacian of Gaussian (LoG) is useful for finding the correct places of edges; however, it is not useful for discovering the orientation of edges because of using the Laplacian filter. Other OC methods like Gaussian based Canny and Shen-Castan have complex computations, false zero crossing and are time consuming [145, 205–207]. Stochastic gradient (SG) [207] shows poor performance in noisy images. The general performance of these methods is subject to the adaptable factors like threshold values and standard deviation. Evaluation of the images demonstrated

Table 3 Comparison of different image segmentation techniques

| No. | References | Year | Method | Type class | Performance measure | Compared to other methods |
|-----|--|--------------|--------------------|------------|---------------------|---------------------------|
| 1 | Ayenu-Prah and Attoh-Okine [14] | 2008 | BEMD* | EBS | C | Yes |
| 2 | Salari and Bao [199], Salari and Ouyang [200] | 2011 | Fractal + Th | TBS | E | No |
| 3 | Huang and Tsai [79] | 2011 | DP-based | RBS | T-A | Yes |
| 4 | Wang et al. [248], [247] | 2007 | Trous + Wavelet | TBS-EBS | V | Yes |
| 5 | Cheng et al. [38], Cai and Zhang [26] | 2001 | Fuzzy set | FBS | V | Yes |
| 6 | Mohajeri and Manning [160] | 1991 | Directional filter | PDE | V | No |
| 7 | Koutsopoulos and Downey [116] | 1993 | Regression Th. | TBS | A | No |
| 8 | Ayenu-Prah and Attoh-Okine [14] | 2008 | BEMD* | EBS | A | Yes |
| 9 | Salari and Yu [201] | 2011 | GA | RBS | A | No |
| 10 | Liu et al. [138] | 2008 | SE* | TBS | V | No |
| 11 | Song et al. [215] | 2015 | RED* | EBS + TBS | A + V | Yes |
| 12 | Jiang et al. [93] | 2015 | Improved EM* | RBS | V | Yes |
| 13 | Golparvar-Fard et al. [63] | 2015 | STFs* | MBS | V | No |
| 14 | Mertz et al. [154], Varadharajan et al. [237] | 2014 | Superpixels | RBS | A + V + T | Yes |
| 15 | Tsai et al. [231] | 2014 | Multiscale CFE* | MBS | V | No |
| 16 | Ying and Salari [272], Ouyang and Wang [182], Ouyang et al. [181] | 2014 | Beamlet | MBS | A + V | No |
| 17 | Lokeshwor et al. [141] | 2014 | ATT* | TBS | A + V + T | Yes |
| 18 | Guan et al. [67] | 2014 | ITVCrack | EBS + MBS | A + V + T + C + I | Yes |
| 19 | Kaul et al. [103, 104], [105], Amhaz et al. [7] | 2014/ 2/0 | EMPS* | MBS | A + V | Yes |
| 20 | Adu-Gyamfi et al. [3], [4] | 2013/ 4 | ACM* | TBS + EBS | V + A + T | Yes |
| 21 | Zuo et al. [299] | 2013 | IFCM* | FBS | V + A | Yes |
| 22 | Zhang et al. [282] | 2013 | MFm* | MBS | V + A | Yes |
| 23 | Xu et al. [264] | 2013 | SSF* | RBS + MBS | V + A | Yes |
| 24 | Na and Tao [164], Xu et al. [262, 264] | 2013/ 2 | ITSM* | TBS | V | No |
| 25 | Tsai et al. [230] | 2013 | GMPBM* | MBS | V + A | No |
| 26 | Tang and Gu [224] | 2013 | HCDsA* | TBS + EBS | V | No |
| 27 | Koutsopoulos et al. [117], Oliveira and Correia [178], Wang and Tang [250, 251], Li [127, 128], Song and Wei [214] | 2013 | Otsu | TBS | V + A | No |
| 28 | Salman et al. [202] | 2013 | 2D Gabor Filter | MBS | V + A | No |
| 29 | Oliveira and Correia [179] | 2013 | Otsu + k-means | TBS + CBS | V + A | No |
| 30 | Li [129], Li et al. [130] | 2013 | ACIGE* | FBS | V | No |
| 31 | Zou et al. [298] | 2012 | TVT* | MBS | V + A | No |
| 32 | Zhang and Zhou [289] | 2012 | Radon + Th | TBS | V + A | No |
| 33 | Wu and Liu [259] | 2012 | DWT* + Th | TBS | V | No |
| 34 | Wang and Gao [244] | 2012 | DT-CWT* | TBS | V + A | Yes |
| 35 | Tsai and Li [234] | 2012 | DOBCS* | RBS | V | No |
| 36 | Tsai et al. [232] | 2012 | AFP* + SPIHT | EBS | V + T | No |
| 37 | Ying and Salari [272], Li [127, 128], Ouyang and Wang [182] | 2012 | Beamlet + Otsu's | TBS + EBS | V | Yes |
| 38 | Nishikawa et al. [173] | 2012 | GP-based* | MBS + RBS | V + A + T | No |
| 39 | Ni et al. [172] | 2012 | BIM* | RBS | V + A + T + C | Yes |
| 40 | Li [127, 128] | 2012 | Contourlet | MBS | V | Yes |
| 41 | Jahanshahi et al. [87], Youquan et al. [274], Huang and Zhang [78], Jahanshahi and Masri [89] | 2012 | MOP* + Otsu's | RBS + MBS | V + A + T | Yes |

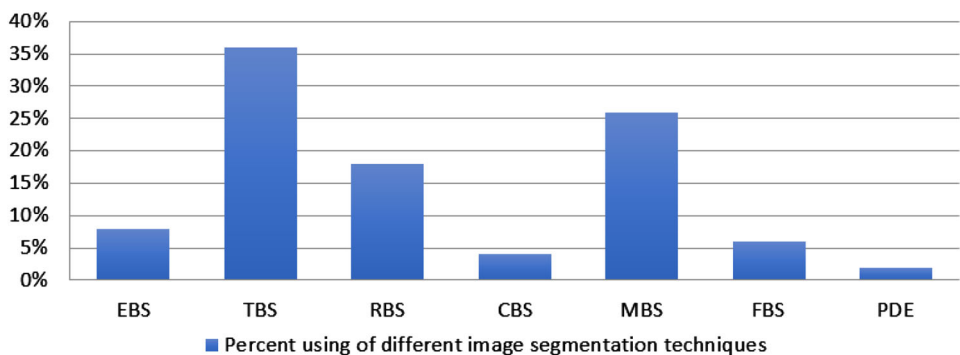
Table 3 continued

| No. | References | Year | Method | Type class | Performance measure | Compared to other methods |
|-----|---|---------------|-----------|------------|---------------------|---------------------------|
| 42 | Moussa and Hussain [163] | 2011 | GCST* | TBS | V + A | No |
| 43 | Salari and Bao [198], Nejad and Zakeri [159] | 2011/ 2010 | Wavelets | MBS + TBS | A | Yes |
| 44 | Li et al. [135] | 2011 | FoS* | RBS | V + A + T + C + I | Yes |
| 45 | Chambon et al. [29] | 2010 | AFMMB* | MBS | V | No |
| 46 | Salari and Bao [199] | 2011 | FFNN* | TBS | V | No |
| 47 | Chambon et al. [29], Chambon and Moliard [30] | 2011 | Markovian | MBS | V + A | Yes |
| 48 | Zhou et al. [293] | 2010 | AT | TBS | V | Yes |
| 49 | Oliveira et al. [176] | 2010 | PDE | CBS | V | Yes |
| 50 | Kaul et al. [103, 104] | 2010 | Hausdorff | TBS | V + A | Yes |

| Performance measure | Method type | Type class |
|-----------------------------|----------------|-------------------------------------|
| T: Time | N: New | EBS: Edge based segmentation |
| C: Computational complexity | E: Enhanced | TBS: Threshold based segmentation |
| I: Iterations | C: Comparative | RBS: Region based segmentation |
| A: Accuracy | | CBS: Clustering based segmentation |
| V: Visual | | MBS: Matching based segmentation |
| | | FBS: Fuzzy based image segmentation |
| | | PDE: Partial differential equations |

BEMD bi-dimensional empirical mode decomposition, *SE** segment extending, *RED** ridge edge detection, *EM** electromagnetism-like mechanism, *STFs** semantic texton forests, *CFE** multiscale crack fundamental element, *ATT** adaptive thresholding technique and user defined decision logic, *EMPS** an enhanced minimal path selection (MPS) algorithm, *ACM** active contours or snake method, *IFCM** an improved fuzzy clustering method, *MFm** matched filtering algorithm, *SSF** saliency and statistical features, *ITSM** iterated threshold segmentation method, *GMPBM** geodesic minimal path based method, *HCDSA** hybrid crack detection and segmentation algorithm, *ACIGE** adaptively changing index via grey entropy, *TVT** tensor voting technique, *DT-CWT** the dual-tree complex wavelet transform, *DOBCS** dynamic optimization-based crack segmentation, *DWT** discrete wavelet transform, *AFP** adaptive filter-bank in lower-level sub-bands, *SPIHT** said pearlman set partitioning in hierarchical trees, *AT** adaptive thresholding, *BIM** biological inspired model, *AFMMB** adapted filtering and markov model-based, *MOP** morphological operation procedure, *FFNN** feed forward neural network, *GCST** graph cut segmentation technique, *FoS* F*Seed-growing, *PDE** parzen density estimation

Fig. 10 Comprehensive comparison of methods used by researchers in recent years



that under noisy conditions (like asphalt pavement), Canny, LOG, Sobel, Prewitt, and Roberts’s reveal better performance, respectively [145, 207].

Huili et al. [82] proposed an improved Canny edge detection procedure and an edge preservation filtering method for pavement edge detection applications. They used Mallat wavelet transform to reinforce the unclear

edges and GA to get a better self-adapting threshold canny algorithm.

Changxia et al. [33] has introduced a method based on FDWT (fractional differential and wavelet transform). This method can effectively enhance high-frequency, medium-frequency signals and non-linearly preserve low-frequency signals. The FDWT is compared with other operators like

Soble, Prewitt and LoG, to demonstrate its performance [179]. The authors concluded that this procedure is effective for different road crack images even in noisy images.

A modified Soble operator is used with bi-dimensional empirical mode decomposition to crack extraction by Ayenu-Prah and Attoh-Okine [14]. Some challenges faced in these sort of approaches for crack detection were false crack edge detection due to the white lane marking, and irregularities in pavement surface, as reported by Oliveria and Correia [179] and Li et al. [135].

Benteli (Bentil and Zhang [11]) presented Multiresolution Information Mining for Pavement Crack Image Analysis. They stated that although some methods or features could have good image edge characteristics, others might show better performance to the special shape and size of objects like crack.

Lokeshwor et al. [140] presents a robust method for automated segmentation of frames with/without distress from road surface video clips based on Canny edge detection. They claimed a method accuracy of up to 96 %.

Tasi et al. [229] stated that the Canny edge detector is the best edge detector among traditional edge detection algorithms. However, the problem is the distress that may seem wider than it actually is and severity of level detection. Therefore, the experimental results show that both accuracy and speed do not meet the requirements.

Mahler et al. [144] used gradient histogram analysis in which the image gradient is highest near an edge of the crack. They employed a sliding mask to calculate the gradient magnitude for each pixel of intensity.

Abdel-Qader et al. [1] presented a comparison of the usefulness of four crack detection methods: Fast Haar Transform (FHT), Fast Fourier Transform, Sobel, and Canny. The outcomes indicated that the FHT was more reliable than the other methods.

The boundary connected the edges to build the shape of an object. They are valuable in the computation of geometry features such as Area, Orientation, Bounding Box, Centerior, Eccentricity, Euler Number, Extent, Extreme, Filled Area, Perimeter, Solidity, Weighted Centerior, and etc.

Connectivity, counter following, edge linking, heuristic graph searching, dynamic programming, and Hough transform are prevalent methods for the analysis of extracted edges. The Hough transform can generalize to detect curves other than straight lines. It can be expressed as Radon transform of a line delta function. One of the functions that can provide local approximations of contours of shape is the B-spline representation function. It is useful in shape synthesis and analysis, graph theory and recognition of parts from boundaries.

Hough transformation is used to detect or classify all cracks in parallel [39]. The experimental results have demonstrated that the cracks are correctly and effectively detected by the proposed method, which will be useful for pavement management.

Nejad and Zakeri [159, 167, 168] presented boundary properties of the peaks to quantify the width and severity of a crack, and the value of a peak to quantify the length and extent of the crack. The volume also covered by the peak is used to serve as a general index for crack quantification (Fig. 12).

The moment's theory provides a useful method to represent the shape of objects as a powerful feature extraction method (MFE). The moments of the region could represent the shape. A crack can be characterized as a point in an N-dimensional vector space. They are useful for shape analysis, and can be used for distress detection, classification, and quantification. Two different types of moments are reported in the references: the n th central moment and n th moment [296]. Zhou et al. [295, 296] reported that when n is 4, the moment could be a good feature for distress detection and isolation. However, it is time consuming and needs a higher speed processor for analysis. When n is 1 it is a good feature for crack detection at the moment. They stated that to detect very small distress it is necessary to choose larger n (1–4) (Fig. 13).

Chou et al. [42] presented a novel approach of applying the theory of fuzzy sets and moment invariants to analyze pavement images. They extracted features based on the theory of fuzzy sets and calculating moment invariants from different types of cracking. They proved the feasibility of using this feature to classify diverse types of pavement cracks.

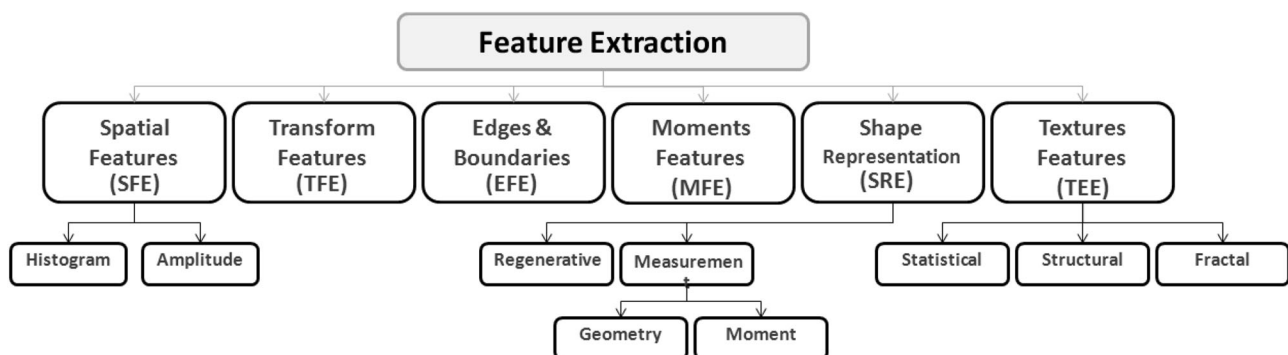


Fig. 11 Image feature extraction methods

In the literature, Rababaah et al. [190] and Hsu et al. used a moment invariant procedure for feature extraction. Feature vectors containing eighteen moments were supplied for classification. Hu, Bamieh, and Zemike moments were some of these moments that were employed for feature generation.

The moments are useful for shape analysis with high speed. A crack can be described by a structure composed of line or curve patterns. Therefore, shape and structure are important for feature extraction. Medial axis transformation, skeleton algorithm, thinning algorithms, morphological processing, and systematic representation are useful for analysis of the structure of cracks [92]. The shape of distress refers to its physical structure. These shapes can be used for crack feature extraction. Several useful shape features are listed in Fig. 10.

In many image based crack analyses, the final goal is to measure certain geometric characteristics based on the shape representation (SRE) of cracks based on previous features, such as: perimeter, area, minimum, and maximum distance, number of hole, Euler number, corners, bending energy, roundness and symmetry.

Many cracks can be represented in terms of moments, such as center of mass, orientation, bounding rectangle, best fit ellipse, and eccentricity. These features are suitable for crack recognition.

The pavement surface as a background of distress is generally random, and it may be coarse, fine, smooth, granulated, rippled, regular, irregular with additional intensified objects like oil, water or shadow. The properties can be changed during the day time and subjected to light and materials. Several statistics that are presented in the references for surface analysis are: the auto colorant function, image transforms, edge density histogram features consisting of [Inertia, mean attribution, variance, and spread distribution] and random texture model (TEE). LeBlanc et al. [122] used the basic fractal characterizations, including the fractal dimension, of some forms of pavement distress.

Pavement images are characterized by a vector of extracted features. These features are then used for the segmentation, detection, or classification steps [298].

The system proposed by Adu-gymfi et al. [4] has three different algorithms for feature extraction: (1) Bi-dimensional empirical mode decomposition (BEMD) and principal component pursuit (PCP), (2) Adaptive thresholding and (3) Active contour models. They combined the BEMD with a crack information mining technique called PCP [2]. The goal was to extract crack information from the different levels or modes of resolution using the BEMD. They concluded that intermediate modes or levels of BEMD hold important crack information.

Traditional pavement detection systems extract crack features by the use of edge detectors and thresholding algorithms which generally work by setting the grey value

of each pixel in the image to a value that is dependent on the magnitude of the gradient of the grey level at the corresponding point in the original image. The processing from this class of systems is purely local. They believed that such systems may be unsuccessful in difficult conditions like rough textures and oil stains [3, 4]. An edge detector method, however does not clearly have the proficiency of recognizing the spreading of the gradients [4].

Since the pavement image texture is very rough, the pavement image surface has foreign objects such as oil stains and paint markings and the image contains a mixture of distress types, and it is difficult to use edge detection or thresholding for feature extraction [4]. The snake method is strong in difficult conditions because of its unique understanding of the edge detection concept. They defined snakes as energy minimizing deformable splines, subjective by limitation and image forces that attract it towards object outlines or borders [4]. These methods are classified into two main classes: the parametric and the geometric active contour models. Parametric models characterize the active contours as parameterized curves. In geometric models, however, they are symbolized as level sets of a two-dimensional function that evolves in an Eulerian framework [3].

Tasi et al. [230] proposed the minimal path method based on the computation of the geodesic distance map $U(x)$ that searches to minimize the weighted distance between two points p_1 and x .

The snake model was also employed by Tang and Gu [224] as a set of discrete points to capture crack borders by diminishing the energy function. In the snake model, the external forces are significant. The general gradient vector flow (GGVF) as the external forces is used, can be obtained by minimizing the following energy function.

The higher order statistics method proposed by Song and Wei [214] is based on the non-homogeneous illumination improvement technique, which improves the image feature considerably. The proposed method is based on the fact that local sections of pavement images have similar geometric texture, and then the probability distribution of image pixel values (PDIPV) in local regions is also similar. This is based on the statement that the feature vector is built by the joint pixel value and the characteristic values of statistical correlation.

Three parametric and three non-parametric supervised classification strategies were presented by Oliveira and Correia [177]. The cracks were then classified to longitudinal, traversal and combined by reconnoitering the 2D feature space [202].

A one-class clustering, using Parzen density estimation, is applied to select cracks, exploiting a simple two dimensional feature space [176]. These features consist of the mean and standard deviation from non-overlapping image blocks.

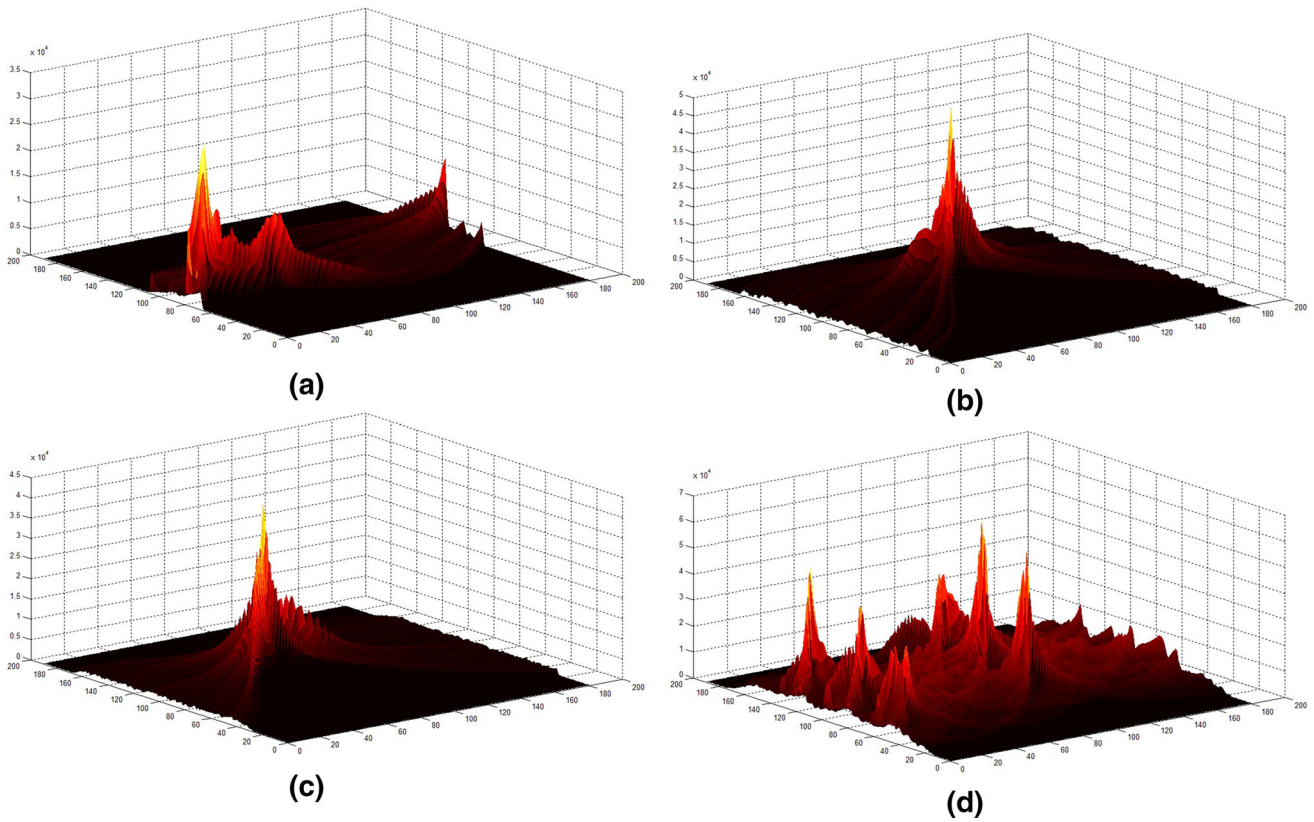


Fig. 12 Three dimensional radon transform (3DRT) reconstruction images, **a** horizontal and vertical cracking, **b** horizontal, vertical and diagonal cracking, **c** block cracking, and **d** alligator cracking [159, 167, 168]

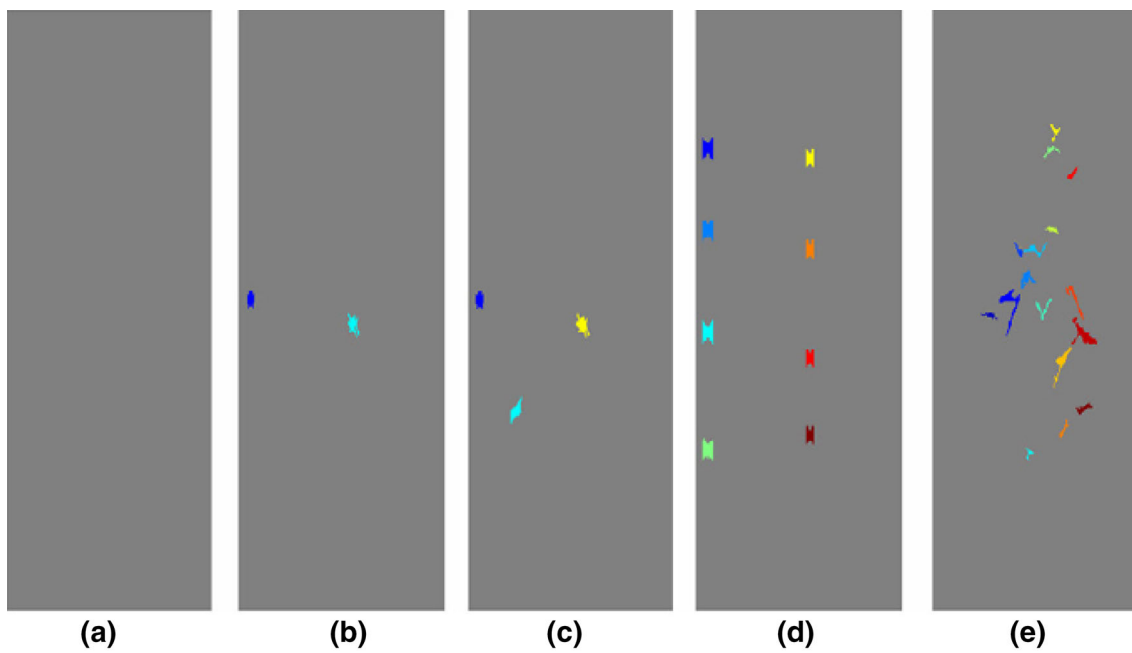


Fig. 13 Binarization of 3DRT and pattern extraction: **a** without cracking, **b** horizontal and vertical cracking, **c** horizontal, vertical and diagonal cracking, **d** block cracking, and **e** alligator cracking [159, 167, 168]

As shown in Fig. 14, among the stated methods, the EFE class is most widely used. According to the study, the frequency of the two TEF and SRE groups in total, is equivalent to using the SEF. According to Fig. 14, more than 50 % of the total approached are EFE and SFE. Also about 23 % of the current approaches are new while the remaining are mostly comparative or enhanced versions of other methods.

According to the above analysis, 57 % of the existing feature extraction techniques are totally used for edges & boundaries extraction and spatial feature extraction. Similar comparisons have also been performed on the originality of feature extraction methods. These comparisons are provided in Fig. 15.

Also about 53 % of the existing approaches are compared with other methods while the remaining 47 % of the methods are not, as shown in Fig. 16.

1.2.4 Feature Selection (FSS)

Although there is inadequate theory to guide in the selection of the best features for crack detection, classification and quantification, it can be stated that some necessary attributes of features are in hand for crack interpretation; and the features should be invariant with translation, scale, and light conditions [163].

The adequacy of feature selection approaches exist in the literature that can be categorized into three groups based on the searching strategy, namely complete search, heuristic search and random search. Feature selection approaches are significant due to dropping computation time, improving the accuracy, decreasing the noise and a better interpretation of the images [31]. Noise and error can be generated using dependent variables and no extra facts, information, and knowledge can be extracted. Reducing the dependent variables can lead to moderating the error and increasing the accuracy in the classification. An appropriate ranking measure is employed to weigh the features and a threshold is selected to reject low weight features [31, 45] (Fig. 17).

Supervised

The effectiveness of features, especially inter feature correlation, is an important criterion to rank a series of features [71, 107, 269]. Ranking methods can be classified into two methods: Correlation criteria, which shows the correlation ranking between variable and goal and Mutual Information, which is an index for measuring the dependency between two variables [16, 31]. Chandrashekar and Sahin [31] classified two ranking techniques as Correlation criteria and Mutual Information to explore the relevance and dependency of a set of features. Various features can be extracted for Pavement distress detection and classification from images. Thus, it can be considered as a

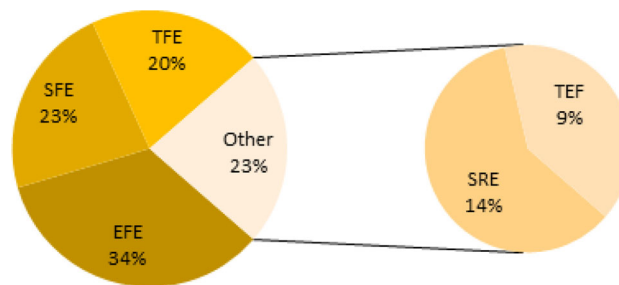


Fig. 14 Comprehensive comparison of methods used by researchers in recent years

multiple variable task. Various methods exist and are proposed by researches for feature selection based on mutual information [12, 24, 49, 75, 97, 139, 217, 254]. Lee and Kim [124] proposed the Mutual Information-based multi-label feature selection method based on interaction information by a measure of dependencies of multiple variables. As a consequence, the proposed method shows good performance for feature selection. A novel feature redundancy index based on mutual information was suggested by Wang et al. [254]. New procedures are proposed to learn feature/kernel weights and NMF parameters by Wang et al. [245]. Jin et al. [97] have used a nonlinear factor for the evaluation function of the feature selection approach. The wrapper procedure shows better performance when the sample size is sufficient.

Hybrid methods (filter-wrapper) show better performance in accuracy and the number of features selected [18, 59, 74, 236]. A hybrid method using the mutual information criterion and a wrapper approach searches in the space for the selection of the candidate feature proposed by Foithong et al. [59]. Huang et al. [76] have proposed a hybrid genetic algorithm to find a subset of features based on two stages consisting of global and local search by using wrapper and filter manners. Zhang and Hu [283] proposed a hybrid feature selection method based on ant colony optimization (ACO) and mutual information. They stated that it can be useful to reduce the dimensionality of the variable, increase the speed of the training and acquire better accuracy. They believed that the hybrid

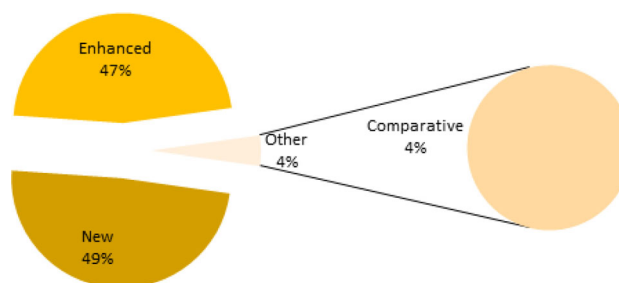


Fig. 15 Categorizing the feature extraction methods based on their originality

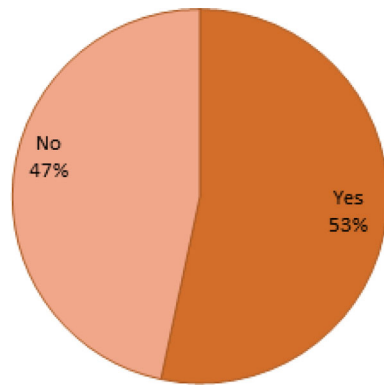


Fig. 16 Classifying the feature extraction methods based on their comparison with other approaches

method shows better performance in both parsimonious feature selection and classification accuracy [18, 54, 59, 74, 76, 283].

Gavilán et al. [61] proposed the best feature vector including diverse texture-based features. The method that they used for feature selection based on the output was provided by the classifier-SVM.

Zhao et al. [290] classified feature selection and extraction techniques into three categories: Fisher score, Principal Component Analysis (PCA), and Laplacian score. Between these three classes, the first one is the supervised method. Based on this method, the score is computed for each discrete feature, and then the highest scores are criteria for selecting those features [290].

Unsupervised

Due to the lack of class labels, unsupervised methods [53, 249, 276] are useful to find an optimal feature vector for data classification (Han et al., [25, 52, 157]). They mined the feature weight matrix and by using pseudo labels, mapped the original data into a low dimensional space. The majority of existing unsupervised feature selection techniques requires prior knowledge of the data and minority work automatically without need for prior

knowledge [119, 266]. PCA and Laplacian score are unsupervised methods that worked by unlabeled data [290].

Maldonado et al. (Maldonado et al.) present an unsupervised method-Kernel K-means—that picks out the most related features, at the same time minimizing the damage of the initial cluster structure and penalizing the use of features via scaling factors (Maldonado et al.).

Previous studies of feature selection are mostly dedicated to supervised and unsupervised approaches. Semi-supervised feature selection is rarely addressed in references. The knowledge from unlabeled and labeled [8] data at the same time exploit using this approach [73, 94, 114, 209]. None of the two methods can take advantage of both labeled and unlabeled points [290]. Supervised and unsupervised feature selection methods need to measure feature weight, however in different ways [291]. Zhao et al. [290] presented a semi-supervised feature selection procedure, which used both labeled and unlabeled data.

Cong et al. [47] used Forward Selection (FS), Backward Selection (BS), Genetic Algorithm (GA) and Principal Component Analysis (PCA) for road distress feature selection. They concluded that PCA is the best method for feature selection when the number of features is larger than 5 [47] and FS is the finest when the number of features is larger than 2 and smaller than 6.

Gavilán et al. [61] stated that the main drawback of methods used for pavement analysis is in the supervised learning group which needs a great amount of data to show good performance [61]. The feature vector included a combination of dissimilar texture-based features. The contour area, bounding box area, fitted bounding box area, contour orientation and the aspect ratio. The idea was to detect blobs with high rectangularity and a wide area inside the bounding box. The AdaBoost algorithm has been employed for choosing Gabor features for the classification of images [279].

Nejad and Zakeri [159, 167, 168] employed the classification accuracies of the dynamic neural network (DNN)

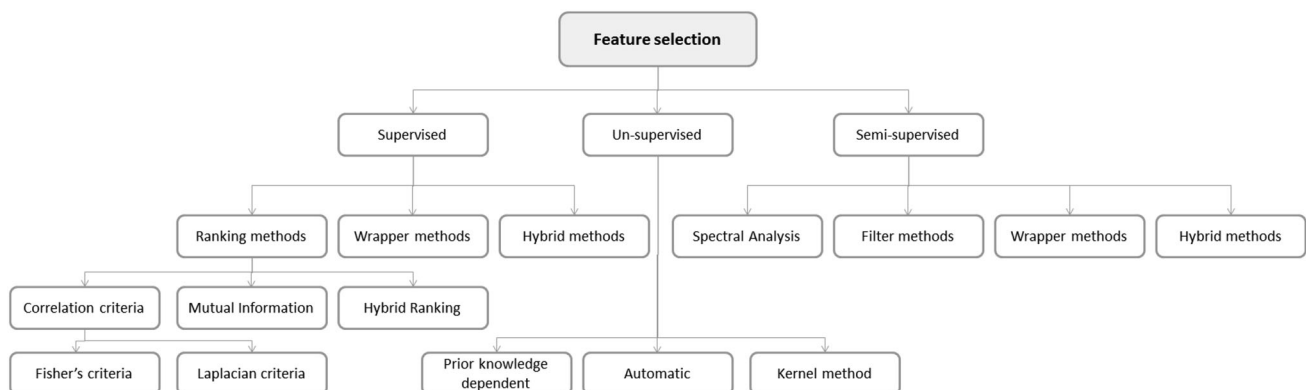


Fig. 17 Feature selection methods

classifier and static neural network (SNN) classifier, as indexes for feature selection.

Table 4 contains the collected information on the studied approaches in the feature selection area. It can be observed that most of the approaches used for feature selection FSs try to use the supervised approaches. These methods mostly develop on basic principles of the error reduction algorithm. On the other hand, similar works on unsupervised feature selection such as Prior knowledge dependent and the Kernel method are rather scarce. This may be based on low accuracy, complexity, and the time of these approaches. We can see that three types of methods based on the concept of ranking methods can be found in the literature. From these three approaches, Hybrid Ranking shows better performance. Therefore, unsupervised and semi-supervised have not received much research attention and except for one new approach, no new work has been done on unsupervised feature selection in recent years. In contrast to unsupervised feature selection, the use of supervised methods is increasing. A portion of these classes among the entire reviewed methods is depicted in Fig. 18.

The pie charts illustrate the feature selection methods based on their originality. They are divided into three parts. 41 % of the total methods are new for feature selection. Also, about 53 % of the existing methods are enhanced while the remaining (6 %) are comparative. In conclusion, we can see that the majority of methods have had positive developments for feature selection.

1.2.5 Detection (DES)

In order to provide good results for automatic systems, it is important to employ objective criteria for distress detection [295, 296]. The first step is the ability to sort images with distress or without defects and then identify distress classes [48].

Various methods have been presented for detecting an isolation of different kinds of distress in pavement surface images [114]. Based on Cord and Chambon [48], research on two major types of tactics have been suggested in the literature for pavement distress detection: (1) Unsupervised methods [175, 179] and (2) Supervised methods [179, 180]. Recently, the semi-supervised method is proposed for using labeled and non-labeled data. The first ones work based on pixels and the second work on classification [48]. In all three supervised, unsupervised and semi-supervised methods, five various approaches can be employed to isolate the images with distress: (1) Statistical Method Based (PMB), (2) Physical Method Based (PMB), Filtering Method Based (FMB), Model-Method Based (MMB), Hybrid Method Based (HMB). In Fig. 13, the various

groups based on different methods are illustrated in three levels.

The Statistical Method Based (SMB) can work based on a wide range of methods like histogram analysis [113, 144], adaptive thresholding [61, 99, 140], thresholding based on fuzzy logic [42], fractal thresholding [200], Gaussian modeling [116, 131, 179], sparse representation [219] kernel tracker [191] Hausdorff distance [233] and invariant moments. These methods are simple but not very efficient because they do not analyze the geometry of cracks [48].

The Physical Method Based (PMB) use morphological tools or contour detection [82, 95, 114, 122, 135]. Crack-Tree [298] and Contourlet transform and multi-direction morphological structuring elements [127, 128] are several examples of this class. These methods consider the constant width and scale for cracking and it is not truthful [48].

The Filtering Method Based (FMB) provides a multi scale platform. Several examples of these methods are the wavelet based method [47, 126, 159, 167–169, 247, 270, 295, 296], Beamlet method [95, 137, 271], contourlet transform [143, 208, 292], shearlet transform [258], ridgelet [285, 286], multi resolution methods [2, 4, 159, 167, 168, 231], filtering based [126, 219–221, 279, 288], average filtering [219–221], Matched filtering [282], adaptive filter-bank [232] or partially different equations, and multi-features [263].

The Model- Method Based (MMB) [48] employed some assumptions related to the geometrics of crack for detection and classification. Some texture decomposition, pattern based, Markova modeling, texture anisotropy measure methods like intra-regional and inter-regional connectivity [263], radon transform [289], minimal paths and dynamic programming [13], Gradient Vector Flow (GVF) [147], Dempster-shafer theory [77] can be considered in this category [135].

The Hybrid Method Based (HMB) is using two or more methods to make a better model for detection and isolation [169, 179, 227, 277, 278].

Cord and Chambon [48] stated that rare classification methods are based on local analysis while local methods are a motivating technique for pavement surface digresses isolation. They proposed an AdaBoost classifier on the multiple descriptor based on PMB and MMB to improve the classification performance [48] (Table 5).

Table 6 The five classes are summarized and researches are cited in the stage of pavement distress detection and isolation.

Zhou et al. stated that all detection methods can be classified into two major classes: edge detection and thresholding. These two categories detect distress in the space domain. However, it is difficult to find a certain

Table 4 Comparison of different feature extraction techniques

| No. | References | Year | Method | Type class | Number of features | Method type compared |
|-----|---|------|---------------------------|------------|--------------------|---------------------------------|
| 1 | Adu-Gyamfi et al. [4] | 2014 | BEMD* + ACM* + AT* | EFE | 3 | N-Yes-[threshold]-(#2)-U |
| 2 | Ayenu-Prah and Attah-Okine [14] | 2008 | BEMD* + Sobel + Canny | EFE | – | C-Yes-(#2 method) |
| 3 | Salari and Bao [199], Salari and Ouyang [200] | 2011 | Radon + Th + Factal | TFE | 2 | E-No-[SVM]-S |
| 4 | Wang et al. [248], [247] | 2007 | Holes algorithm | EFE | – | N-Yes |
| 5 | Cheng et al. [38], Cai and Zhang [26] | 2001 | Fuzzy set | EFE | 4 | N-Yes-[reasoning]-S |
| 6 | Salari and Yu [201] | 2011 | GA | SRE | 4 | E-No-[NN]-S |
| 7 | Song et al. [215] | 2015 | RED* | SFE | 8 | N-Yes-[reasoning]-(#1)-S |
| 8 | Jiang et al. [93] | 2015 | Improved EM* | TEF | 2 | E-Yes-[SFEA]-(#4)-U |
| 9 | Golparvar-Fard et al. [63] | 2015 | STFs* | SRE | 2 | N-No-[STFC] -S |
| 10 | Tsai et al. [231] | 2014 | Multiscale CFE* | EFE | 5 | N-No-[reasoning]-U |
| 11 | Ying and Salari [272], Ouyang and Wang [182], Ouyang et al. [181] | 2014 | Beamlet | TFE | 3 | E-No-[reasoning]-S |
| 12 | Lokeshwor et al. [141] | 2014 | ATT* | EFE | 1 | E-Yes-[logic]-(#2)-S |
| 13 | Guan et al. [67] | 2014 | IGRF* | EFE | 5 | E-Yes-[threshold]-(#2 Method)-S |
| 14 | Adu-Gyamfi et al. [3], [4] | 2014 | BEMD* + PCP* + AT* + ACM* | TFE | – | E-Yes-[-(#2)-U |
| 15 | Tsai et al. [230] | 2013 | GMPBM* | SFE | 3 | N-No-[-(#0)-U |
| 15 | Tang and Gu [224] | 2013 | HCDSA* | SFE + MFE | 4 | E-Yes-[threshold]-(#1)-S |
| 16 | Koutsopoulos et al. [117], Oliveira and Correia [178], Wang and Tang [250, 251], Li et al. [131, 132], Song and Wei [214] | 2013 | INCP* | TFE | 3 | N-Yes-[SVM]-(#1)-S |
| 17 | Salman et al. [202] | 2013 | 2D Gabor Filter | TFE | 6 | N-No-[logic]-(#0)-S |
| 18 | Oliveira and Correia [179] | 2013 | Otsu + k-means | SFE | 2 | N-No-[threshold]-(#0)-U |
| 19 | Zou et al. [298] | 2012 | TVT* | SRE | 4 | N-Yes-[threshold]-(#4)-S |
| 20 | Zhang and Zhou [289] | 2012 | MFA* | SRE | – | E-No-[logic]-(#0)-S |
| 21 | Wang and Gao [244], Wu and Liu [259] | 2012 | DT-CWT* | TFE | 3 | E-Yes-[threshold]-(#1)-S |
| 22 | Tsai and Li [234] | 2012 | DOBCS* | SFE | – | N-No-[threshold]-(#0)-S |
| 23 | Tsai et al. [232] | 2012 | AFP* + SPIHT | TEF | 3 | N-No-[threshold]-(#0)-US |

Table 4 continued

| No. | References | Year | Method | Type class | Number of features | Method type compared |
|-----|---|--------|-----------------------|------------|--------------------|---------------------------------------|
| 24 | Ying and Salari [272], Li [127, 128], Ouyang and Wang [182] | 2012 | Beamlet +Otsu's | TFE | 3 | N-Yes-[threshold]-(#3)-S |
| 25 | Nishikawa et al. [173] | 2012 | GP-based* | TFE | 4 | E-No-[threshold]-(#1)-S |
| 26 | Ni et al. [172] | 2012 | BIM* | SFE | 4 | E-No-[adaboost]-(#1)-S |
| 27 | Li [127, 128] | 2012 | Contourlet | EFE | 2 | E-Yes-[threshold]-(#3)-S |
| 28 | Jahanshahi et al. [87], Youquan et al. [274], Huang and Zhang [78], Jahanshahi and Masri [89] | 2012 | MOP* + Otsu's + Cany | EFE | 5 | C-Yes-[NN, SVM, Ne-neighbor]-(#3)-S,U |
| 29 | Moussa and Hussain [163] | 2011 | GCST* | SFE | 7 | N-No-[SVM]-(#0)-S |
| 30 | Nejad and Zakeri [159] | 2011 | Multi-resolution | TFE | 7 | E-Yes-[NN]-(#2)-S |
| 31 | Salari and Bao [198], Nejad and Zakeri [159] | 2011 | Wavelets | SFE | 2 | N-No-[logic]-(#0)-S |
| 32 | Li et al. [135] | 2011 | FoS* | EFE | 2 | N-No-[logic]-(#3)-U |
| 33 | Salari and Bao [199] | 2011 | FFNN* | SFE | - | E-No-[NN]-(#0)-U |
| 34 | Chambon et al. [29] | 2010 | AFMMB* | EFE | - | N-Yes-[Markov]-(#3)-U |
| 35 | Song et al. [215] | 2015 | RED* | EFE | 6 | N-No-[threshold]-(#0)-U |
| 36 | Varadharajan et al. [237] | 2014 | Superpixels | TEF | 138 | N-No-[SVM]-(#0)-U |
| 37 | Guan et al. [67], [66] | 2014 | ITVCrack + GRF* | SRE | 2 | E-Yes-[logic]-(#3)-S |
| 38 | Amhaz et al. [7] | 2014 | EMPS* | EFE | 2 | E-Yes-[]-(#4)-U |
| 39 | Zuo et al. [299] | 2013 | IFCM* | SRE | 2 | E-Yes-[FCM]-(#2)-U |
| 40 | Xu et al. [264] | 2013 | SSF* | SFE | 2 | E-Yes-[bayesian]-(#6)-U |
| 41 | Na and Tao [164], Xu et al. [262, 264] | 2013/2 | ITSM* | EFE | 2 | E-No-[logic]-(#0)-S |
| 42 | Song and Wei [214] | 2013 | Statistics Properties | TEF | 8 | E-Yes-[SVM]-(#1)-S |
| 43 | Li et al. [130] | 2013 | Gray Entropy | EFE | | N-No-[]-(#0)-U |

Performance measure

Feature extraction techniques

T: Time

SFE: Spatial features extraction

C: Computational

TFE: Transform features extraction

Complexity

EFE: Edges and boundaries extraction

I: Iterations

MFE: Moments features extraction

A: Accuracy

SRE: Shape representation extraction

Table 4 continued

| Performance measure | Feature extraction techniques |
|---------------------|-----------------------------------|
| V: Visual | TEF: Textures features extraction |
| Method type | |
| N: New | |
| E: Enhanced | |
| C: Comparative | |

*SFLA** shuffled frog-leaping algorithm, *GRF** geo-referenced feature, *BEMD** bi-dimensional empirical mode decomposition, *PCP** principal component pursuit, *AT** adaptive thresholding, *ACM** active contour model, *INCP** illumination non-uniformity correction principle, *MFA** matched filtering algorithm, *GRF** geo-referenced feature, *EMPS** an enhanced minimal path selection (MPS) algorithm

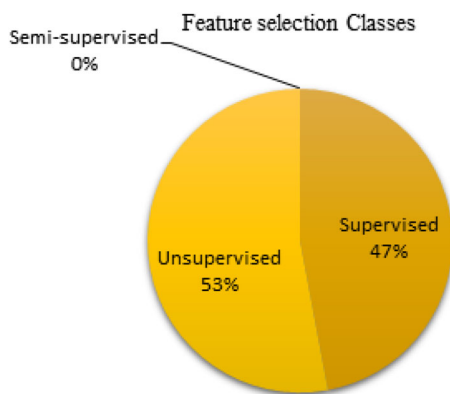


Fig. 18 Ratio of feature selection classes (supervised, unsupervised and semi-supervised)

threshold to detect a distress for these methods. They use wavelet domain instead of using the space domain for distress detection. Several criteria including the High-Amplitude Wavelet Coefficient Percentage (HAWCP), the High Frequency Energy Percentage (HFEP), the Standard Deviation (STD) and moments of wavelet coefficient (MWC) were used based on wavelet coefficient in the high-frequency-sub bands of the wavelet domain [295, 296]. These quantities were meaningful and effective for pavement fault detection and isolation.

Changxia et al. [33]. proposed a new approach of pavement cracks isolation based on fractional differential and wavelet transform (FDWT). Fractional differential can effectively enhance various frequencies. Then wavelet transform is applied in order to strain noise. Experimental results proved that the proposed detection was a valid method for the different road crack images even if no noise exists.

Gavilán et al. [61] used a seed-based approach for crack detection, combining Multiple Directional Non-Minimum Suppression (MDNMS) with a symmetry check which is classified in MMB crack detection methods. Several parameters are used to adjust the method. Seeds are linked by computing the paths with the lowest cost that meet the

symmetry restrictions. For the entire detection, they started it to get optimal results without manual intervention and correct setting played an important role [61] (Figs. 19, 20).

Overall, as it can be seen from Fig. 21, unsupervised and supervised types were the main approaches of distress detection and isolation, whereas the semi-supervised type was not used in this regard.

According to the above analysis, 55 % of the approaches are designed for SMB and FMB, and the remaining are proposed in PMB, MMB and HMB. Similar comparisons have also been made for the reader in the realm of detection and isolation. These comparisons are provided in Figs. 22 and 23.

1.2.6 Classification (CLS)

Machine learning methods are frequently used for pavement distress segmentation and classifications [114, 152, 159, 167, 168, 190, 200, 208, 219, 229, 247, 250, 251, 271, 272, 277, 288]. These procedures distinguish the variances between crack and non-crack regions, and also different types of distress, severities and extent. Diverse classification approaches have been proposed for different applications [114, 161]. Very few studies have been carried out to evaluate diverse classification methods [161]. On the other hand, limited approaches have been used for detection of pavement cracks from images and classifying the type, severity and extent which can be categorized based on Fig. 14: Artificial neural networks (ANN), [13, 21, 39, 41, 101, 102, 123, 171, 189, 197, 229, 260, 261], Fuzzy and adaptive neuro-fuzzy inference system (ANFIS) [20, 36–38, 225], Support Vector Machine (SVM) [61, 88, 134, 136, 148, 164, 200, 222], decision trees [159, 167, 168, 295], Chain code [243], k-nearest neighbors [91, 101], Parzen windows [177], Fisher's Least Square Linear classifiers [177], Genetic algorithm [201], Multiple Instance Learning [237], AdaBoost [48], Metaheuristic methods [172], and Bayes [32].

Table 5 Comparison of different distress detection and isolation techniques

| No. | References | Year | Method | Type class | Descriptor | Compared to other methods |
|------------|--|--------------------------|-------------------------------|------------|------------|---------------------------|
| 1 | Jiang et al. [93] | 2015 | Unsupervised | TEF | Global | Yes |
| 2 | Song et al. [215] | 2015 | Unsupervised | HMB | Global | No |
| 3 | Adu-Gyamfi et al. [3], [4] | 2014 | Unsupervised | HMB | Global | Yes |
| 4 | Lokeshwor et al. [141] | 2014 | Unsupervised | PMB | Global | Yes |
| 5 | Guan et al. [67] | 2014 | Supervised | HMB | Global | Yes |
| 6 | Varadharajan et al. [237] | 2014 | Unsupervised | HMB | Global | Yes |
| 7 | Amhaz et al. [7] | 2014 | Unsupervised | PMB | Local | Yes |
| 8 | [4] | 2008 | Supervised | PMB | Local | Yes |
| 9 | Changxia et al. [33] | 2009 | Supervised | FMB | Global | No |
| 10 | Gavilán et al. [61] | 2011 | Unsupervised | MMB | Global | Yes |
| 11 | Moussa and Hussain [163] | 2011 | Supervised | SMB | Global | No |
| 12 | Salari and Bao [198] | 2010 | Supervised | SMB | Global | No |
| 13 | Nejad and Zakeri [159] | 2011 | Supervised | SMB | Global | Yes |
| 14 | Li et al. [135] | 2011 | Unsupervised | FMB | Global | Yes |
| 15 | Chambon et al. [29] | 2010 | Unsupervised | FMB | Global | Yes |
| 16 | Zuo et al. [299] | 2013 | Unsupervised | MMB | Global | Yes |
| 17 | Xu et al. [264] | 2013 | Unsupervised | SMB | Global | Yes |
| 18 | Na and Tao [164], Xu et al. [262, 264] | 2013/2 | Supervised | SMB | Global | No |
| 19 | Tsai et al. [230] | 2013 | Unsupervised | PMB | Local | No |
| 20 | Tang and Gu [224] | 2013 | Supervised | HMB | Local | No |
| 21 | Song and Wei [214] | 2013 | Supervised | SMB | Local | Yes |
| 22 | Salman et al. [202] | 2013 | Unsupervised | FMB | Global | No |
| 23 | Song and Wei [214] | 2013 | Supervised | SMB | Local | Yes |
| 24 | Oliveira and Correia [179] | 2013 | Unsupervised | SMB | Global | Yes |
| 25 | Li [129], Li et al. [130] | 2013 | Unsupervised | FMB | Local | No |
| 26 | Zuo et al. [299] | 2013 | Unsupervised | SMB | Local | Yes |
| 27 | Zou et al. [298] | 2012 | Unsupervised | HMB | Local | Yes |
| 28 | Zhang and Zhou [289] | 2012 | Unsupervised | FMB | Global | No |
| 29 | Wang and Gao [244] | 2012 | Supervised | FMB | Local | Yes |
| 30 | Tsai and Li [234] | 2012 | Supervised | PMB | Global | No |
| 31 | Tsai et al. [232] | 2012 | Unsupervised | FMB | Global | No |
| 32 | Ouyang and Wang [182] | 2012 | Supervised | FMB | Local | Yes |
| 33 | Nishikawa et al. [173] | 2012 | Supervised | FMB | Local | No |
| 34 | Ni et al. [172] | 2012 | Supervised | MMB | Global | Yes |
| 35 | Li [127, 128] | 2012 | Supervised | FMB | Local | Yes |
| 36 | Jahanshahi and Masri [89] | 2012 | Supervised | MMB | Local | Yes |
| Descriptor | Method type | | Type class | | | |
| Local | Supervised | | SMB: Statistical method based | | | |
| Global | Unsupervised | | PMB: Physical method based | | | |
| | Semi-supervised | | FMB: Filtering method based | | | |
| | | | MMB: Model-method based | | | |
| | | HMB: Hybrid method based | | | | |

Table 6 Comparison of different classification techniques for pavement distress classification

| No. | References | Year | Method | Type class | Descriptor | Compared to other methods |
|-----|---|------------------|--------|------------|---------------|---------------------------|
| 1 | Jiang et al. [93] | 2015 | USL | NI | – | Yes |
| 2 | Song et al. [215] | 2015 | USL | DT | – | No |
| 3 | Adu-Gyamfi et al. [4] | 2014 | USL | LC | – | Yes |
| 4 | Guan et al. [67] | 2014 | SL | LC | – | No |
| 5 | Lokeshwor et al. [141] | 2014 | USL | DT | Logic | No |
| 6 | Varadharajan et al. [237] | 2014 | USL | SVM-MIL | LIBSVM | Yes |
| 7 | Amhaz et al. [7] | 2014 | USL | LC | – | Yes |
| 8 | Nguyen et al. [171] | 2009 | SL | NN | BP | No |
| 9 | Oliveira and Correia [179] | 2013 | USL | LC-DT-HC | – | Yes |
| 10 | Lee and Lee [123], Ceylan et al. [28] | 2004, 2014 | SL | NN | – | No |
| 11 | Zhou et al. Zhou et al. [295], [296] | 2003, 2005, 2006 | SL | DT | CART | No |
| 12 | Salari and Ouyang [200] | 2012 | SL | SVM-DT | – | No |
| 13 | Avila et al. [13] | 2014 | USL | LC | DP | No |
| 14 | Bray et al. [21] | 2006 | SL | NN | BEMD | No |
| 15 | Tsai et al. [231] | 2014 | USL | DT | – | No |
| 16 | Ouyang et al. [181] | 2014 | SL | DT-LC | CIT | No |
| 17 | Zakeri et al. [277] | 2013 | SL | NN-DT | – | No |
| 18 | Oliveira and Correia [179] | 2013 | USL | LV | – | No |
| 19 | Wang and Gao [244] | 2012 | SL | LC | – | Yes |
| 20 | Gavilán et al. [61], Na and Tao [164] | 2012 | SL | SVM | PSVM | No |
| 21 | Wang and Feng [252] | 2012 | SL | DT | – | No |
| 22 | Salari and Yu [201] | 2012 | SL | NN | – | No |
| 23 | Nejad and Zakeri [159, 167, 168] | 2011 | SL | NN | DNN | Yes |
| 24 | Gavilán et al. [61] | 2011 | SL | SVM | LSVM | No |
| 25 | Moussa and Hussain [163] | 2012 | SL | SVM | Kernel | No |
| 26 | Salari and Bao [198] | 2010 | SL | LC | LV | No |
| 27 | Nejad and Zakeri [159] | 2011 | SL | DT | – | No |
| 28 | Li et al. [135] | 2011 | USL | – | – | Yes |
| 29 | Salari and Bao [199] | 2011 | SL | NN | – | No |
| 30 | Chambon et al. [29] | 2010 | USL | BC | – | Yes |
| 31 | Zuo et al. [299] | 2013 | USL | FC | Logic | Yes |
| 32 | Xu et al. [264] | 2013 | USL | BC | Bayesian | Yes |
| 33 | Na and Tao [164], Xu et al. [262, 264] | 2013/2 | SL | LV | Interpolation | No |
| 34 | Tsai et al. [230] | 2013 | USL | DT | Logic | No |
| 35 | Tang and Gu [224] | 2013 | SL | DT | – | Yes |
| 36 | Koutsopoulos et al. [117], Oliveira and Correia [178], Wang and Tang [250, 251], Li et al. [131, 132], Song and Wei [214] | 2013 | SL | SVM | Kernel | No |
| 37 | Salman et al. [202] | 2013 | USL | DT | – | No |
| 38 | Oliveira and Correia [179] | 2013 | SL | LC | Logic | No |
| 39 | Li [129], Li et al. [130] | 2013 | USL | FC | – | |
| 40 | Zou et al. [298] | 2012 | USL | DT | MST* | Yes |
| 41 | Zhang and Zhou [289] | 2012 | SL | DT | PC | No |
| 42 | Tsai and Li [234] | 2012 | SL | DT | DO* | No |
| 43 | Tsai et al. [232] | 2012 | USL | LC | – | No |

Table 6 continued

| No. | References | Year | Method | Type class | Descriptor | Compared to other methods |
|-------------------------------|----------------------------------|--|--------|------------|------------|---------------------------|
| 44 | Ouyang and Wang [182] | 2012 | SL | – | – | No |
| 45 | Nishikawa et al. [173] | 2012 | SL | – | – | No |
| 46 | Ni et al. [172] | 2012 | SL | BC | Adaboost | No |
| 47 | Li [127, 128] | 2012 | SL | – | – | Yes |
| 48 | Jahanshahi and Masri [89] | 2012 | SL | SVM/LC/NN | SVM/NN | Yes |
| Method | Type class | ID3: Iterative Dichotomiser 3 | | | | |
| SL: Supervised learning | SVM: Support vector machines | C4.5: Successor of ID3 | | | | |
| USL: Unsupervised learning | LC: Linear classifiers | CART: Classification and regression tree | | | | |
| SSL: Semi-supervised learning | KE: Kernel estimation | CHAID: CHi squared automatic interaction detector | | | | |
| RL: Reinforcement learning | BC: Boosting classifier | MARS: Extends decision trees to handle numerical data better | | | | |
| DL: Deep learning | NN: Neural networks | CIT: Conditional inference trees | | | | |
| HL: Heuristic learning | LV: Learning vector quantization | FLI: Fisher's linear discriminate | | | | |
| | DT: Decision trees | LR: Logistic regression | | | | |
| | QC: Quadratic classifiers | NBC: Naive Bayes classifier | | | | |
| | FC: Fuzzy clustering | PC: Perception | | | | |
| | | LSSVM: Least squares support vector machines | | | | |
| | | KNN: k-nearest neighbor | | | | |
| | | RF: Random forests | | | | |
| | | DP: Dynamic programming | | | | |
| | | BEMD: Bidimensional empirical mode decomposition | | | | |
| | | PSVM: Proximal support vector machine | | | | |
| | | DNN: Dynamic neural network | | | | |
| | | LSVM: Linear SVM | | | | |
| | | MST: Minimum spanning trees | | | | |
| | | DO: Dynamic-optimization | | | | |
| | | MIL: Multiple instance learning | | | | |

A comparison of these methods and using the most predictive classifier is very important and difficult. Each of the methods shows diverse effectiveness and correctness based on the kind of datasets. The criteria for evaluation will be discussed in Sect. 1.3.

This section briefly reviews the various classification approaches used in order to categorize the pavement surface images into various distress, severities and extent.

An unsupervised two-step pattern recognition method is presented in [179]. Based on the unsupervised procedure, six clustering methods consisting of hierarchical, k-means and hybrid (two Gaussians) were considered for training. The outcome was the image blocks without crack pixels or with crack pixels [179]. Also, the crack type characterization rules are used for classification of longitudinal (L), transversal (T) and miscellaneous (M) cracks. They reported that all detected cracks were correctly classified as

three types of L, T, and M. The best overall performance was 93.5 % for F-measure, recall was 95.5 % and the best global error rate was 0.6 %.

Chou et al. [41, 42] proposed the theory of fuzzy sets and used moment invariants from different types of distress for pavement distress detection and classification. Then, a back-propagation neural network was used as a classifier.

The BP is employed by Nguyen et al. [171] for automatic detection and classification of defects on road pavement using anisotropy measures.

In order to classify crack types of digital pavement images, Lee et al. [123] proposed an integrated neural network-based crack imaging system. The proposed system is used as three neural networks: image-based neural network, histogram-based neural network, and proximity-based neural network. Integrated NNs are used to classify

Categorizing the feature extraction methods based on their originality

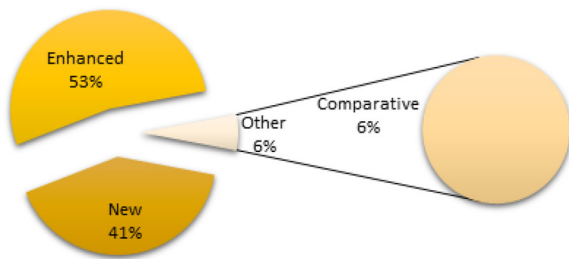


Fig. 19 Categorizing the feature selection methods based on their originality

various crack types based on the tiles. The proximity-based neural network effectively searches the patterns of various crack types. The accuracy of 95.2 % is reported for pavement distress classification.

Zhou et al. [295, 296] used a two-step transformation method by wavelet and radon transform to determine the type of the crack. According to this method, several statistical criteria are developed in distress detection and isolation, which include the High-Amplitude Wavelet Coefficient Percentage (HAWCP), the High-Frequency Energy Percentage (HFEP), and the Standard Deviation (STD). These criteria are tested on hundreds of pavement

images differing by type, severity, and extent of distress. Experimental results demonstrate that the proposed criteria are reliable for distress detection and isolation and that real-time distress detection and screening is feasible based on supervised DT learning [296]. However, the proposed method still suffers from (1) the effects of noise which are generated by the asphalt concrete surface and low quality of cracks (which is lower than 2 % information), (2) thresholding method (crisp) and (3) classification procedure. Therefore, these three areas have become the scope of work for many researchers in recent years.

Hsu et al. [74] described a moment invariant technique for feature extraction and a NN for crack classification. The moment invariant technique reduces a two dimensional image pattern into feature vectors that characterize the image such as: translation, scale, and rotation of an object in an image. Then the neural network in which back-propagation learning was used in its training, classifying this feature, attempted to produce the desired output. However, the back-propagation neural network [159, 167, 168, 295, 296] may be used to provide fitness against noise. The results that they reported showed that moment invariant and the neural network can be considered as a robust technique for accurate classification in various types of airport pavement distress [48, 85].

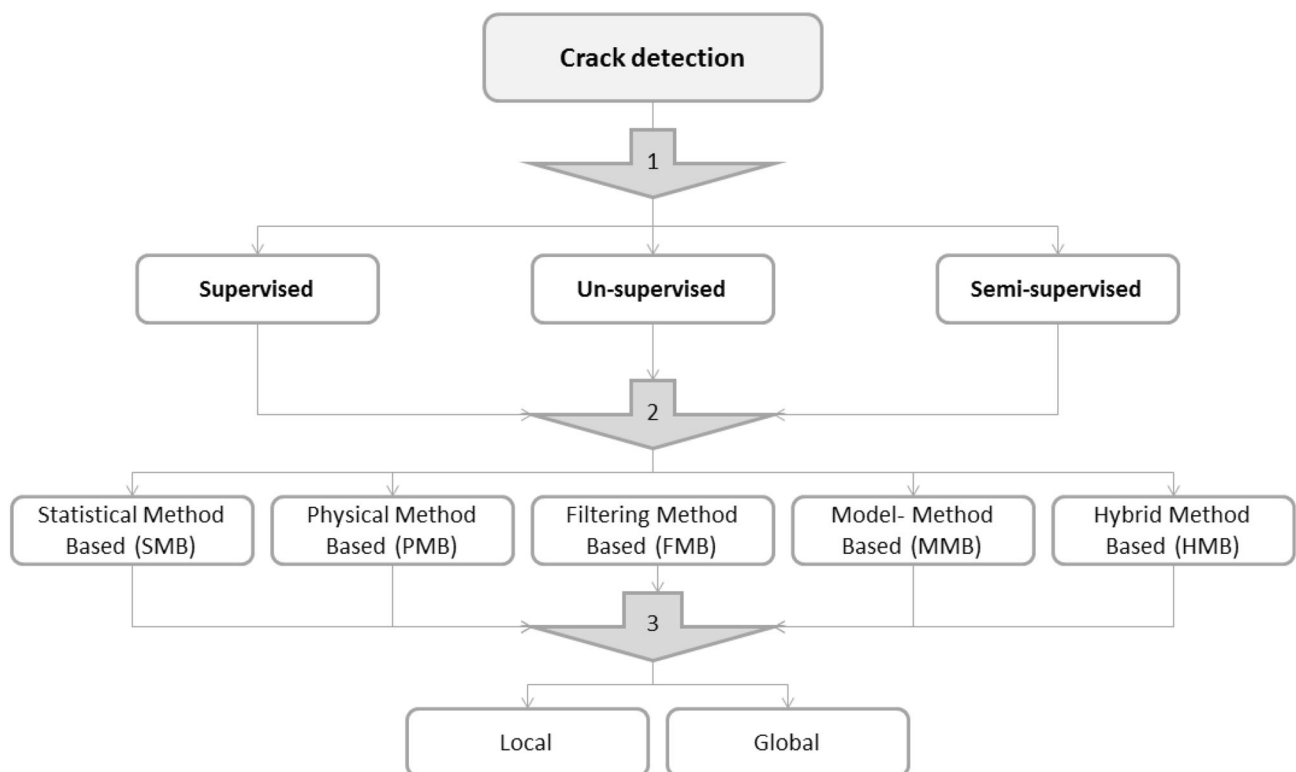


Fig. 20 Classification of crack detection methods based on: 1 supervised, unsupervised and semi-supervised, 2 statistical method based (SMB), physical method based (PMB), filtering method based

(FMB), model-method based (MMB), hybrid method based (HMB), 3 local and global [48, 250, 251]

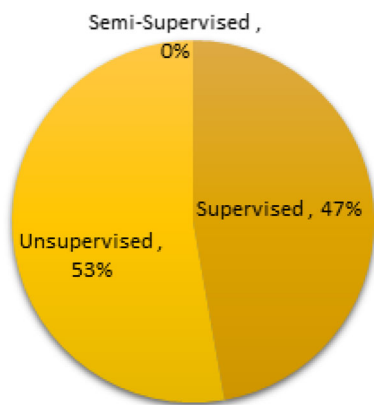


Fig. 21 Comparison of different distress detection and isolation methods

Salari and Ouyang [200] used a three step method for distress classification based on SVM. In the first step, they employed a Support Vector Machine to classify the image. Then they used fractal thresholding in order to isolate the cracks. Finally, to classify the cracks they used Radon Transform based on DT to classify the specific crack type [200]. To train the classifier, a total of 40 samples are used. The successful rate of the proposed approach is about 95 for segmentation and over 90 % for classification [200].

Avila et al. [13] proposed a new technique for crack segmentation based on finding the minimal path passing on each pixel of the image. They propose a dynamic programming implementation in real conditions. The results demonstrated the ability of the proposed method for isolation cracks as small as 2 mm [13].

Bray et al. [21] also proposed a classification method based on NN for automatic classification of road cracks. The NN works according to features that are extracted from density and histogram. The features are passed to a NN for the classification. The next NN is employed for the classification of a crack type.

Nejad and Zakeri [159, 167, 168] used a method for Optimum Feature Extraction Based on Wavelet–Radon Transform and Dynamic Neural Network for Pavement

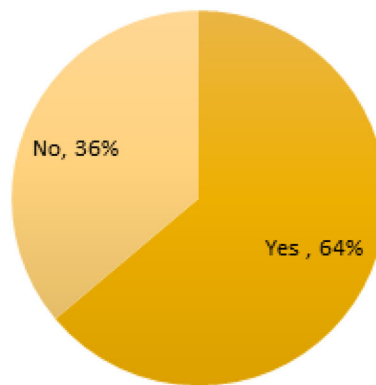


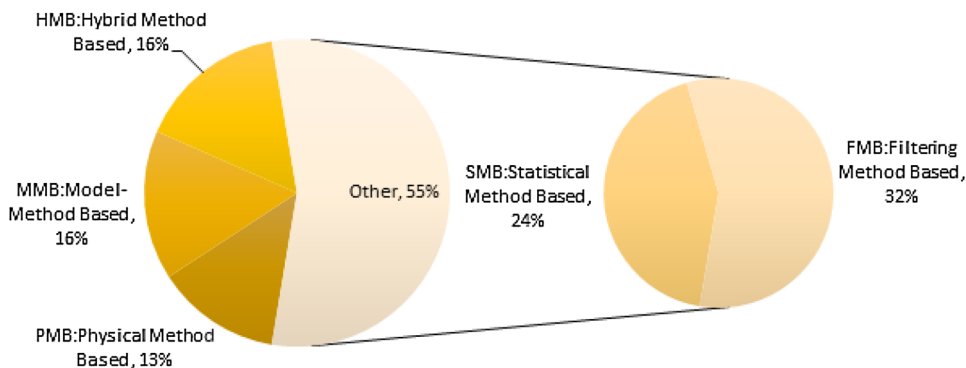
Fig. 23 Ratio of distress detection and isolation compared techniques

Distress Classification. This research demonstrated that the WR + DNN method can be used efficiently for fast automatic pavement distress detection and classification. Dynamic Neural Network (DNN) Threshold selection is used for accuracy of the proposed method. A two-dimensional (2D) extension of EMD is used for pavement distress images. A bi-dimensional intrinsic mode function (BIMF) is employed and the authors reconstruct a composite image by selecting salient information from coarse and fine resolution BIMFs useful for accurate extraction of linear patterns in a pavement distress image. The methodology used in this paper reported better results [2].

Tasi et al. [231] presented a novel crack fundamental element (CFE) approach based on a multiscale topological crack representation. The proposed multiscale CFE model makes available properties of crack that can be employed to develop new crack classification approaches to describe cracks and create a flexibly model for crack classifications [231].

Ouyang et al. [181] proposed the Beamlet algorithm to analyze the pavement crack images and classify the four different cracks based on direction. The Beamlet algorithm has a good robustness for the reason that its line detection was suitable for crack detection and classification algorithm. The proposed method can detect the transverse crack

Fig. 22 Comparison type classes of different distress detection and isolation techniques



and longitudinal crack by 100 %, and alligator crack and block crack by above 85 % [181].

Zakeri et al. [277] presented a multi-stage expert system for pavement cracking isolation and classification. The Combination of Wavelet modulus and 3D Radon Transform are employed for knowledge generation. Finally, an NN is used for classification of distress [277].

Nejad and Zakeri developed an automatic diagnosis system for isolation and classification of pavement cracks based on Wavelet–Radon Transform (WR) and Dynamic Neural Network (DNN) threshold selection. The algorithm of the proposed system consists of a combination of feature extraction using WR and classification using the neural network technique. The proposed WR + DNN system performance is compared with the static neural network (SNN) [159, 167, 168].

Two classifiers are used for detection and classification by Olivera et al. [179] for crack detection and then classification which is based on learning from the samples paradigm, unsupervised training. Also, a new procedure for crack severity levels evaluation is presented [179].

Wang and Goa [244] presented dual-tree complex wavelet transform (DT-CWT) for pavement distress identification. It used a multi-scale and multi-resolution approach to decompose a pavement image into multi-level sub-bands, with high frequency sub-bands containing distress [244]. The experimental study outcomes established its performance enhancement over Discrete Wavelet Transform (DWT) [244].

Na and Tao [164] proposed an approach for automatic classification of pavement surface images. The proximal support vector machine (PSVM)—enhanced classifier—is employed for pavement distress classification, which is more efficient and easier to be implemented than the traditional support vector machine. The experimental results prove that the computation efficiency and classification performance both show better results. The standard PSVM, a variant of SVM, is established based on the optimization concept by Mangasarian, etc. Related with SVM, the method not only improves the computation efficiency but also improves the classification performance. They reported that the classification accuracy rate of the PSVM was 91.15 %. [164].

Wang and Feng [252] proposed the shearlet frame for filtering the pavement images. In the classification of operation, they used the classification rules extracted from Radon transform for crack and angle detection and used scattering distance to verify the result of classification by the texture feature of pavement distress images [252].

Salari et al. [201] used a three-layer feed-forward neural network for a type classification. Based on their method, the vertical and horizontal distress measures along with the total number of distress tiles are then used in NN [201].

The author also used a neural network based pavement distress classifier using the geometrical parameters obtained from the distresses. Simulation results are given to show that the proposed method is both effective and reliable on a variety of pavement images [199].

Figure 24 compares the classification methods for three categories namely Supervised learning (SL), Unsupervised learning (USL) and Semi-supervised learning (SSL). It is clear that the largest proportion of methods went to SL. On the other hand, Semi-supervised (SSL) has the lowest percentage in the chart. A portion of these categories compared to other classifiers is depicted in Fig. 25. According to the above analysis, 69 % of the existing classification methods are not compared with other procedures.

1.3 Image Interpretation Group (IIG)

The number of published papers dealing with crack detection and classification of pavement distress rapidly increased in the previous years. The majority of methods with respect to automatic asphalt pavement evaluation, is concentrated on detection and classification of distress. There is no general and robust automatic method at hand to determine the severity and extent of the level of visual cracking. There are rare indications or quantities in methods assigned to the severity and extent of detected and classified pavement distress.

In [179], a new method is proposed for assigning the severity level of each type of cracks. This method works based on the subset of distress type and width of the crack. Since the calculation of the width of a crack is a difficult task for various widths and directions, the average width of a crack is used to quantify the severity levels. The average width of the cracks can be estimated based on the total number of pixels in a crack to the total number of pixels in the cracks skeleton [179]. However, this method is not excellent at severity assigning for very thin cracks (<2 mm width).

Zhou et al. [296] developed three statistical criteria for distress detection and isolation, which include HAWCP, HFEP and STD, based on wavelet analysis. A norm form cracking quantification based on HAWCP and HFEP was proposed and the usefulness of the proposed indexes is demonstrated. According to this research, the HAWCP parameter for the wavelet at the first level is a high-quality measure for the extent of cracking representation. HFEP, as a good index for severity, is defined as the energy of high-frequency segmented image over the total energy of a pavement image. Also, they believed that one of the best methods to quantify the severity of the cracking section based on wavelet coefficients is to quantify the energy of the coefficients. Distresses are transformed into high-

frequency sub-bands, and the high—amplitude wavelet coefficient has more energy than low—amplitude [296]. The spread of the wavelet coefficients shows the worse pavement conditions. Zhou proposed several simple statistical parameters that facilitate explaining and analyzing the histogram. Finally, pavement distress quantification (PDQ) was proposed as a general index combined of severity and extent and defined $PQD = HAWP * HFEP$. Based on their research, HAWCP, HFEP and STD proved to be effective criteria for real-time distress detection and quantifying [159, 167, 168, 295, 296].

Additionally, Zhou et al. [295, 296] found relationships between the pattern of peaks and properties of cracks (type, severity and extent). Based on their research, the number of peaks can be used to determine the type of cracks as single or multiple cracks [295]. Based on the RT rules, the position of RT is related to the orientation and position of cracks. The areas of peaks are related to the width of cracks and can be used to determine the severity of cracks. The peak value shows a good relationship between the value of RT and the extent of cracking distress [295].

The pattern of peaks are used for training the neural network to classify the type of crack and the factors of the peaks are employed to quantify the severity and extent of the crack [159, 167, 168]. Under some circumstances, the intensity of the background may be close to the distress, and sometimes there can be some tiny, thin cracks. To solve this problem, a new approach is proposed. For a peak in RT number, position, area, value and volumes are used for knowledge extraction. Nejad and Zakeri used an area of the peaks to quantify the width and severity of a crack, and the value of a peak to quantify the length and extent of the crack. Also, they used the volume of the segmented area as a general index for crack quantification. As a conclusion, they found that some statistical parameters are independent measures for the extent and severity of distress and some of

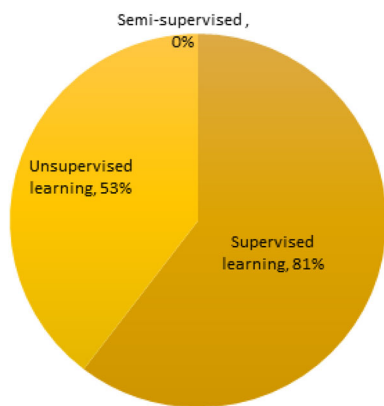


Fig. 24 Comparison of different classification techniques for pavement distress classification based on Supervised learning (SL), Unsupervised learning (USL) and Semi-supervised (SSL)

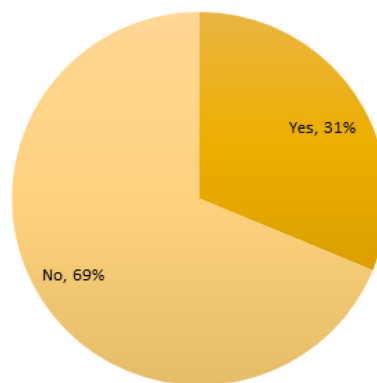


Fig. 25 Compared to other methods

them are subjective. The area of a peak can be selected to quantify the width and severity of a crack and the value of the peak can be used to measure the length and extent of the crack. For the block or alligator cracks, the entire area of the pavement affected by the cracking can be representative of the severity level. The Cumulative Radon Transform (CRT) and Dynamic thresholding are proposed for quantification.

2 Performance Evaluations

To determine the overall performance of a method, a wide variety of well-known metrics for evaluation purposes have been used in the last two decades. The current inspection activity of the pavement surface depends mainly upon the inspectors, technologies, soft computing method, visual inspection, and feeling with distress. This inspection activity could be very subjective and highly dependent on expert opinion.

The reliability and effectiveness of automatic systems are difficult to evaluate especially for different conditions. There are many indexes such as mean square error (MSE), mean absolute error (MAE), entropy, index of fuzziness, mean square error, and peak signal to noise ratio to evaluate the performance. However, accuracy is not a reliable and robust index for the real evaluation of the classifier, because it will yield misleading results if the data set is unbalanced (that is, when the number of samples in different classes vary greatly).

In this section, we classified statistics methods into four classes: General statistics, basic ratios, ratios of ratios, and Additional statistics. From the confusion matrix Accuracy, Error, Probability of detection, Selectivity, Reproducibility, Negative Predicted Value (NPV), False Positive Rate (FPR), False Negative Rate (FNR), False Discovery Rate (FDR), False Omission Rate (FOR), Likelihood Ratio for

Positive Tests (LRPT), Likelihood Ratio for Negative Tests (LRNT), Likelihood Ratio for Positive Subjects (LRPS), Likelihood Ratio for Negative Subjects (LRNS) are computed. Additional statistics like F-measure, balanced accuracy, Matthews Correlation Coefficient (MCC), Chisq: χ^2 , Difference between Automatic and Manual classification, Dissimilarity Index of Bray Curtis are used to compare the results. The general performance has been evaluated according to the vector measures extracted from the confusion matrix.

$$\begin{aligned} \text{Accuracy} &= \frac{(TP + TN)}{(TP + TN + FP + FN)} \\ \text{Error} = 1 - \text{Accuracy} &= 1 - \frac{(TP + TN)}{(TP + TN + FP + FN)} \\ \text{TPR} = \text{Recall} = 1 - \text{FNR} &= \frac{TP}{TP + FN} \\ \text{TNR} = \text{Specificity} = 1 - \text{FPR} &= \frac{TN}{TN + FP} \\ \text{PPV} = \text{Precision} = 1 - \text{FDR} &= \frac{TP}{TP + FP} \\ \text{NPV} = 1 - \text{FOR} &= \frac{TN}{TN + FN} \\ \text{FPR} = 1 - \text{Specificity} &= \frac{FP}{FP + TN} = \text{Type I error} \\ \text{FNR} = 1 - \text{Recall} &= \frac{FN}{TP + FN} = \text{Type II error} \\ \text{FDR} = 1 - \text{Precision} &= \frac{FP}{TP + FP} = q - \text{Value} \\ \text{FOR} = 1 - \text{NPV} &= \frac{FN}{FN + TN} \\ \text{LRPT} = \frac{\frac{TP}{TP+FN}}{\frac{FP+TN}{FP+TN}} &= \frac{\text{Recall}}{1 - \text{Specificity}} = \frac{\text{Recall}}{\text{FPR}} \\ \text{LRNT} = \frac{\frac{FN}{FN+TP}}{\frac{TN+FP}{TN+FP}} &= \frac{(1 - \text{Recall})}{\text{Specificity}} = \frac{\text{FNR}}{\text{Specificity}} \\ \text{LRPS} = \frac{\frac{TP}{TP+FP}}{\frac{FN+TN}{FN+TN}} &= \frac{\text{Precision}}{(1 - \text{NPV})} = \frac{\text{Precision}}{\text{FOR}} \\ \text{LRNS} = \frac{\frac{FP}{FP+TP}}{\frac{TN+FN}{TN+FN}} &= \frac{(1 - \text{Precision})}{(1 - \text{FOR})} = \frac{\text{FDR}}{\text{NPV}} \\ \text{Fmes} = \text{F - measure} = \text{F1} &= 2 * \frac{(\text{Precision} * \text{Recall})}{(\text{Precision} + \text{Recall})} \\ \text{BalAcc} = \frac{(\text{Recall} + (1 - \text{FPR}))}{2} &= \frac{(\text{Recall} + \text{Specificity})}{2} \end{aligned}$$

$$\begin{aligned} \text{MCC} &= \frac{(TP * TN) - (FP * FN)}{((TP + FP) * (TP + FN) * (TN + FP) * (TN + FN))^{0.5}} \end{aligned}$$

$$\begin{aligned} \text{Significance} = \text{Chisq} : \chi^2 &= \frac{[(TP * TN) - (FP * FN)]^2 * (TP + TN + FP + FN)}{(TP + FP) * (TP + FN) * (TN + FP) * (TN + FN)} \end{aligned}$$

$$\text{Auto}_{\text{Manu}} = (TP + FP) - (TP + FN)$$

$$\begin{aligned} \text{Dissimilarity Index of Bray Curtis} &= \frac{|(\text{Auto}_{\text{Manu}})|}{\sum(TP + FP) + \sum(TP + FN)} \end{aligned}$$

In contrast to FPR = (1 - Specificity), the True Positive Rate (1 - FNR) provides meaningful knowledge about the relevant correctly identified samples. Recall is also sometimes called sensitivity. A test with a high recall and specificity has low type II and type I error rates. The F1-Score or harmonic mean of precision is a hybrid index made of both Precision and Recall. Sensitivity shows the potential of positive recovery rate and complementarity, and the specificity measures the potential of negative recovery rate. The MCC is a powerful index with a range of 1 for perfect correlation and -1 for negative correlation and value 0 for a random prediction. Balanced Accuracy (BalAcc) is a more robust index to compare results of the in balanced data set.

The performance of repeatability or reproducibility enables us to evaluate the performance by the Positive Predicted Value (PPV).

An additional analysis of performance, based on Ratios of Ratios and Additional statistics, can be used for performance evaluation of the methods. The following measures were calculated: Likelihood Ratio for Positive Tests, Likelihood Ratio for Negative Tests, Likelihood Ratio for Positive Subjects, Likelihood Ratio for Negative Subjects, F-measure, Balanced Accuracy, Matthews Correlation Coefficient, and Difference between automatic and manual classification, Dissimilarity Index of Bray Curtis, Discriminate Power, Youdens Index.

Also, Receiver Operating Characteristics (ROC) graphs have been used for checking and visualizing the performance of the methods [55]. This method is able to create a better measure for evaluation of a method than the scalar method such as Type BR, ROR or AS metrics.

A Scoring Measure (ScM) index is proposed based on the Hausdorff distance metric to estimate the crack detection algorithm ability. It has a value between 0 and 100, with ScM of 100 points to the most precise outcomes.

Table 7 Comparison of different indexes to evaluate the performance

| No. | References | Year | Method | Speed | Types performance evaluations | | |
|-----|---|------|---------------|-------|-------------------------------|---------------------------|------|
| | | | | | BR | ROR | AS |
| 1 | Jiang et al. [93] | 2015 | UM | R | – | – | – |
| 2 | Grandsaert [64] | 2015 | SM | R | TPR, PPV | – | Fmes |
| 3 | Song et al. [215] | 2015 | SM | R | Acc, FDR, FOR | – | – |
| 4 | Varadharajan et al. [237] | 2014 | ROC | R | PPV, TPR | – | – |
| 6 | Lokeshwor et al. [141] | 2014 | SM | R | Acc, PPV, TPR, Error | – | – |
| 7 | Guan et al. [67], Guan et al. [66] | 2014 | SM | S | Acc | – | – |
| 8 | Amhaz et al. [7] | 2014 | SM | S | – | – | Fmes |
| 9 | Adu-Gyamfi et al. [4] | 2014 | SM | S | – | – | Fmes |
| 10 | Oliveira and Correia [179] | 2013 | SM | S | PPV, Acc, FOR, Error, Acc | LRPT, LRNT, LRPS and LRNS | Fmes |
| 11 | Salari and Ouyang [200] | 2012 | SM | S | TPR, Acc | LRNT, LRNS | – |
| 12 | Ouyang et al. [181] | 2014 | SM | R | TPR, Acc | – | – |
| 13 | Jahanshahi and Masri [89] | 2012 | SM | S | Acc, TPR, TNR, PPV | – | – |
| 14 | Moussa and Hussain [163] | 2011 | SM | S | ACC | – | – |
| 15 | Salari and Bao [198] | 2010 | SM | R | ACC | – | – |
| 16 | Nejad and Zakeri [159] | 2011 | SM | R | Acc, TPR, TNR, PPV | – | – |
| 17 | Li et al. [135] | 2011 | SM | S | PPV, TPR | – | Fmes |
| 18 | Chambon et al. [29] | 2010 | SM | NI | TPR, TNR | – | Fmes |
| 20 | Zuo et al. [299] | 2013 | SM | S | Acc | – | – |
| 21 | Xu et al. [264] | 2013 | ROC | NI | PPV, TPR, Error | – | Fmes |
| 22 | Na and Tao [164], Xu et al. [262, 264] | 2012 | SM | NI | Error | – | – |
| 23 | Tsai et al. [230] | 2013 | SM | R | PPV, TPR, Error | – | – |
| 24 | Tang and Gu [224] | 2013 | SM | NI | FOM* | – | – |
| 25 | Koutsopoulos et al. [117], Oliveira and Correia [178], Wang and Tang [250, 251], Li et al. [131, 132], Song and Wei [214] | 2013 | SM | NI | Acc, Error | – | – |
| 26 | Salman et al. [202] | 2013 | SM | NI | TPR, PPV | – | – |
| 27 | Li [129], Li et al. [130] | 2013 | SM | NI | – | – | – |
| 28 | Golparvar-Fard et al. [63] | 2015 | SM | NI | Acc | – | – |
| 29 | Tsai et al. [231] | 2014 | SM | NI | Acc, PPV | – | – |
| 30 | Zou et al. [298] | 2012 | SM | S | TPR, PPV | – | Fmes |
| 31 | Zhang and Zhou [289] | 2012 | SM | NI | Acc | – | – |
| 32 | Wang and Gao [244] | 2012 | GS (PSNR) | NI | – | – | – |
| 33 | Tsai and Li [234] | 2012 | GS (PSNR&ScM) | R | – | – | – |
| 34 | Tsai et al. [232] | 2012 | GS (PSNR&SM) | R | – | – | – |
| 35 | Ouyang and Wang [182] | 2012 | GS (SNR), SM | NI | Acc | – | – |
| 36 | Nishikawa et al. [173] | 2012 | SM | NI | Error | – | – |
| 37 | Ni et al. [172] | 2012 | SM | R | Acc | – | – |
| 38 | Li [127, 128] | 2012 | GS (PSNR), SM | NI | Acc | – | – |

Method

Speed

ROC: Receiver operating characteristics

S: Slow

SM: Statistics metrics

R: Real-time

NI: No information

Type performance evaluations

Table 7 continued

| Method | Speed |
|--|-------|
| GS: General statistics | |
| BR: Basic ratios | |
| ROR: Ratios of ratios | |
| AS: Additional statistics | |
| Type BR | |
| Acc: Accuracy | |
| Error = 1 – Acc | |
| TPR: True positive rate | |
| TNR: True negative rate | |
| PPV: Positive predicted value | |
| NPV: Negative predicted value | |
| FDR: False discovery rate | |
| FOR: False omission rate | |
| Type ROR | |
| LRPT: Likelihood ratio for positive tests | |
| LRNT: Likelihood ratio for negative tests | |
| LRPS: Likelihood ratio for positive subjects | |
| LRNS: Likelihood ratio for negative subjects | |
| Type AS | |
| F-measure (Fmes) | |
| Balanced accuracy (BalAcc) | |
| Matthews correlation coefficient (MCC) | |
| Chisq (χ^2) or significance | |
| Difference between automatic and manual classification (AutoManu) | |
| Dissimilarity index of bray curtis (DIBC) | |
| Discriminate power ((DIP), 1 \approx Poor, 3 \approx Good, Fair \approx Otherwise) | |
| Youdens index (YOI) | |

$$ScM = \left(100 - \left(\frac{BH(x_i, y_i)}{w} \right) \right) \times 100$$

where the BH (x_i, y_i) is the distance between two sections, and w is the recommended 0.2*width of the image [234] (Table 7).

The following pie chart shows the amount of assessment from different categories of performance evaluations. As is observed from the given data, the Basic Ratios (BR) made remarkable progress in performance evaluations over Table 8 (Figs. 26, 27).

At first glance, it is clear for BR that the biggest slice of the pie chart is devoted to Table 8 which is 74 % (Fig. 28). However, less effort was spent on ROR that was 5 %.

Overall, it can be deduced that fewer studies were accounted for ROR by researchers. Moving to a further description, it is vivid that more researches are needed for quality control and assurance of methods.

Figure 29 illustrates the results of the presented survey about the speed and time of the methods. It is clear that based on the survey results, most of the methods have no information about time analysis and the complexity of algorithms.

2.1 Protocols

A computerization-oriented protocol for conditions of asphalt surface pavements was developed in 1996 by FHWA [70]. The standards of ASTM and AASHTO revealed principles for pavement condition evaluation [70]. (AASHTO R 55 and AASHTO PP 67 and AASHTO PP 68). The severity of cracking was overestimated based on the AASHTO standard protocol [193]. Various indexes are proposed to assess the asphalt pavement condition [81, 246, 253].

3 Emerging and Evolution Technologies and Future Works

The prior sections have given a general review on automatic asphalt pavement surface distress evaluation under the title of three groups: Image Acquisition Group (IAG), Image Processing Group (IPG) and Image Interpretation Group (IIG), for the latest.

Table 8 List of of different future and emerging technologies in the field of asphalt pavement distress detection, classification and evaluation

| Number | Research and development | Status | Potential application | Related article |
|--------|--|---------------------------|--|---|
| 1 | Satellite | R and E and P | Remote sensing, less expensive, very fast, and cover wider areas | Jin and Davis [98], Zarrinpanjeh et al. [281], Li et al. [133], Paraforos et al. [184] |
| 2 | QUAV | H and R and D and E and P | Remote sensing, high resolution, near real-time imagery less expensive, more consistent, fast, and cover wide section, careful inspection, programmable assessment, flexible, maneuverable | Montero et al. Metni and Hamel [155], Leong et al. [125], Zhang and Elaksher [284], Colomina and Molina [46], Michaelsen and Meidow [156], Siebert and Teizer [212], Vasuki et al. [239], Grandsaert [64], Schnebele et al. [203] |
| 3 | BCI, neuro prosthetics, Neuromorphic | H and R | Rapid pavement assessing, expert knowledge extraction, Control judgment in the assessment | Gerson et al. [62], Luo et al. [142], Gao et al. [60], Iacoviello et al. [83], McCane et al. [150], Nguyen et al. [170], Rouillard et al. [196], Wirkner et al. [257], Asensio-Cubero et al. [9], Atkinson and Campos [10], Files and Marathe [58], Rai and Deshpande [192] |
| 4 | Behavior-based robots (BBR) and Artificial brain | H | Expert decision simulation, analysis based on meta-knowledge, transfer knowledge to intelligent agent and robots, need no programming | Burattini et al. [22], Kupferberg et al. [120], Fernandez-Leon et al. [57] |
| 5 | Swarm robotics (cloud robotics) | H and E | Autonomous audit, pavement distress detection, classification and quantification, knowledge generation and learn from each other agents | Guenard and Ciarletta [68], Tong et al. [228], Jiménez-González et al. [96], Natalizio et al. [166], Tan and Zheng [223], Wei et al. [255], McCune and Madey [151], Qureshi and Koubâa [188], Varela et al. [238], Aghaeeyan et al. [5], Kostavelis and Gasteratos [115], Kruglova et al. [118], Yao et al. [266–268], Bayindir [17], Senanayake et al. [204], Shukla and Karki [211], Shukla and Karki [211] |
| 6 | Hybrid (FPV and UAV and BCI) | H | Autonomous inspection, pavement distress recognition, quantifies distress, knowledge generation and learns from experts brain signals | Kim et al. [108] |
| 7 | Nanorobotics | H | could be employed to inspect, repair and healing cracks | Verma and Chauhan [241] |
| 8 | Kirilan photography (Aura) | H | Detection of vital energy of pavement, prediction to propagate surface distress | Duerden [50, 51], Hubacher [81], Prakash et al. [186] |

R research, *D* development and diffusion, *E* experiments, *P* prototypes, *H* hypothetical

In this section, research opportunities with an emphasis on emerging technologies and innovative approaches are discussed. In real environments with regards to different characteristics of asphalt pavement, the use of existing systems that cannot work properly are costly and time consuming. In addition, the parameter of engineering judgment is not considered for existing automatic systems and the knowledge generation by these systems is impossible.

One possible solution for solving the problem could be the use of a satellite or UAV platform as a remote sensing technology for data collection and automatic inspection of the pavement surface.

Images taken from the satellites platform, make available the largest spatial coverage of roads and are used in a wide range of applications. Due to this low spatial

resolution, they are still not suitable for road studies. However, it is predicted that in the near future they are equipped with high resolutions and make them a great platform for automatic pavement assessment.

Quadcopter Unmanned Aerial Vehicles (QUAV) are a good platform for making high quality imagery with more maneuverability than both manned aerial platforms (MAP) and unmanned aerial vehicles (UAV). Their short time to answer extraordinary movements, and dynamic resolutions make them a great platform for pavement inspection missions.

These platforms create a new chance to cover large areas in little time. These technologies will create an occasion to decrease the sections number and size depending on the visits.

With the advent of tiny robot inspection, assessment and repair of the pavement could be changed in the near future.

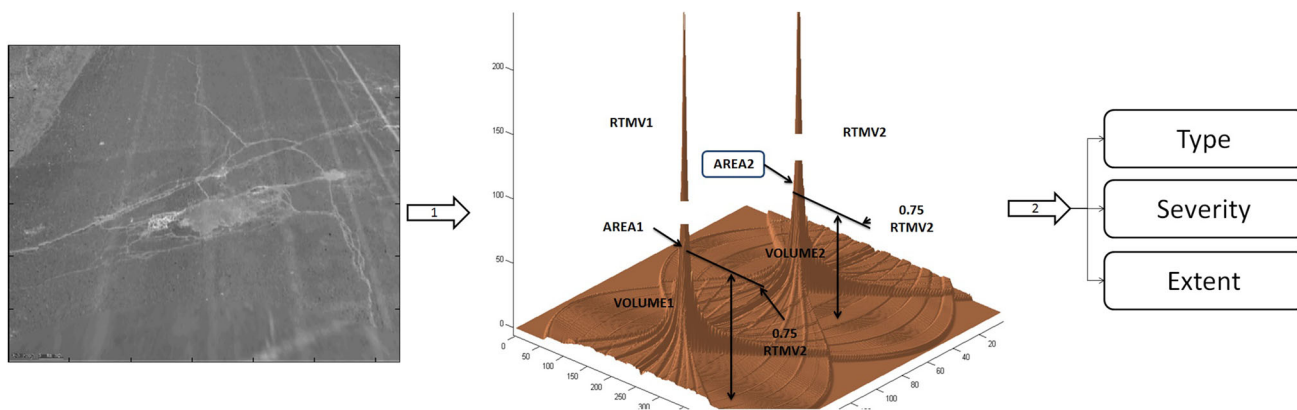


Fig. 26 A peak in radon domain and its parameters [159, 167, 168, 295]

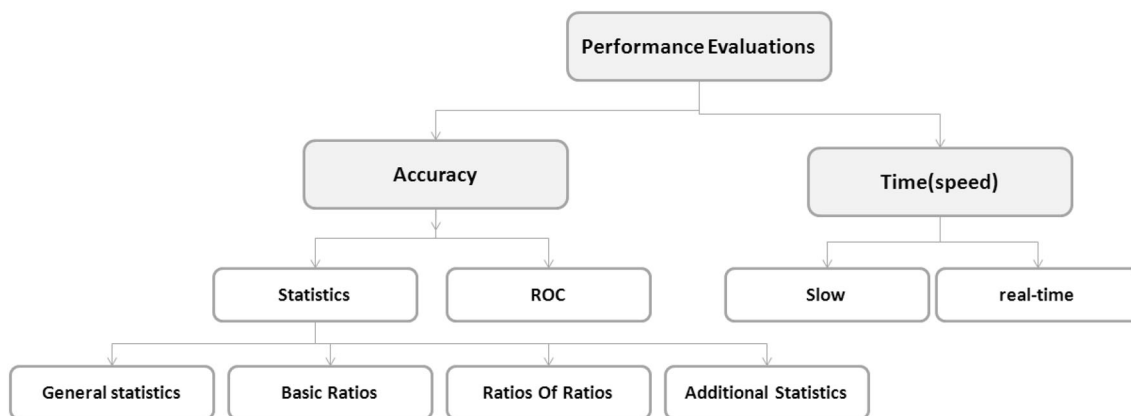


Fig. 27 Classification of metrics for evaluation purpose of pavement distress detection and classification consists of: accuracy and time. The accuracy split in two groups of statistics (general statistics, basic

ratios, ratios of ratios, and additional statistics) and receiver operating characteristics (ROC)

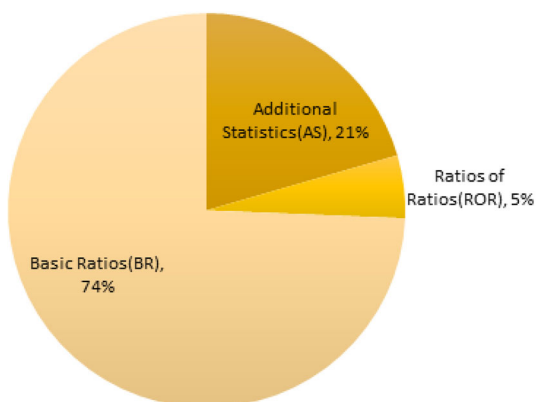


Fig. 28 Categorizing the types of performance evaluations based on their indexes

Nanorobotics are considered as the emerging automata in the scale of $\leq 10^{-9}$ m [241]. One of the valuable applications of Nano machines might be inspection of pavement. For instance, repairs-nano robots could be employed to inspect, repair and heal cracks.

A stimulating topic for future field studies is represented by transferring the swarm robotics discipline to the micro and nano-scale. Swarms of tiny robots can be employed for pavement network management through the inspection and assessment of distress, maximizing the frequency and accuracy of inspection and minimizing the cost for pavement repairing aims. Several challenges for starting and using these tools are presented in [17].

It is demonstrated that computer vision systems and image processing procedures have to be less successful

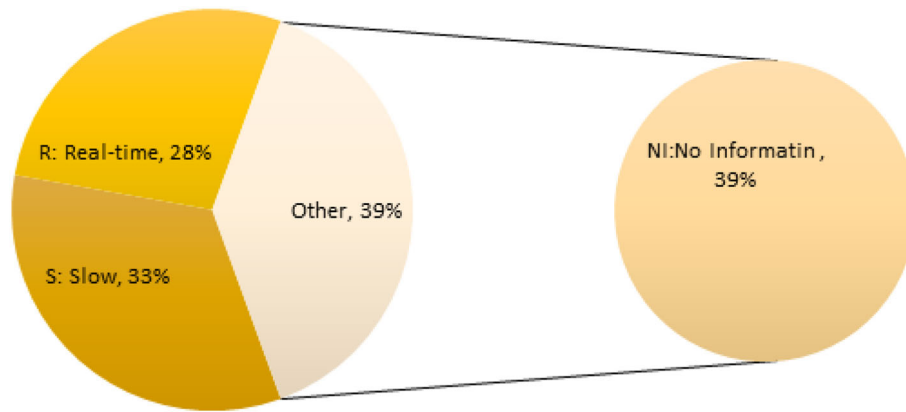


Fig. 29 Determination of different methods in terms of speed

than human visual interpretation [62]. An encouraging topic for future inspection and assessment is brain computer interface “BCI” as an emerging NDT technology. It does not require different sensors or complex algorithms. An electroencephalography (EEG) system capable of identifying neural signatures of visual recognition events was evoked during rapid serial visual presentation (RSVP).

Since the BCI and RSVP method enables inspectors to rapidly analyze facts and figures over a wide section, it has come to be an interesting technique for evaluating distress in infrastructure and pavements. Using BCI for the analysis of infrastructure is a novel and different exploration agenda.

An automatic remote assessment of pavement using an intelligent Quadcopter agent (QUAV) with a low cost electroencephalogram (EEG) headset, like Emotic Epoc, is our mission for the next decade.

4 Summary

It is significant to assess and quantify distress at a regular period. Usually, such evaluations are accomplished as visual, semi-automatic, and automatic approaches. Recently, automated and semi-automated pavement assessment and evaluation has received more and more attention. The appearances of type, severity, and extent of pavement surface cracking are the main features to evaluate the condition of asphalt pavements. The condition assessment results are used to predict future conditions, to support investment planning, and to allocate limited maintenance and repair resources.

This research has studied the current efforts of evaluating the automatic/semi-automatic asphalt pavement distress detection and classification under the headings of: Image Acquisition Group (IAG), Image Processing Group (IPG) and Image Interpretation Group (IIG).

In the first part of this paper, diverse types of automatic/semi-automatic systems are reviewed. Industrialization of these platforms are very costly and the quality of consequences are extremely subject to employed sensors. Therefore, in order to improve the quality of images taken from the pavement, more powerful (intelligent, high quality and low cost) tools are required. It is concluded that nearly all commercial systems need a powerful illumination system to prepare uniform lighting conditions for capturing images. Therefore, in order to improve the quality of images taken from the pavement, a more powerful device is needed. The use of robotics quickly increased in many fields of civil engineering because of its benefits (safety, efficiency, and quality).

The second part of the paper has concentrated more on a comprehensive synthesis of the state of the art in the Image Processing Group (IPG). A framework has been proposed for pavement distress detection and classification. Several methods have been categorized, and literature on Pre-Processing (PPS), Segmentation (SEP), Feature Extraction (FES), Feature Selection (FSS), Detection (DES), Classification (CLS) and Image Interpretation Group (IIG) have been presented.

The third part of this paper has focused on parameters and indexes to evaluate the overall performance of a method. There are many methods used to evaluate the performance. However, the current inspection activity of the pavement surface depends on many parameters. A universal synthesis of the cutting-edge in parameters and indices to evaluate models has been summarized in this part.

Finally, future and evolution technologies have been introduced to enhance both the platform and the analysis for future research.

Compliance with Ethical Standards

Conflict of interest The authors declare that they have no conflict of interest.

References

- Abdel-Qader I, Abudayyeh O, Kelly ME (2003) Analysis of edge-detection techniques for crack identification in bridges. *J Comput Civ Eng* 17(4):255–263
- Adu-Gyamfi Y, Okine NA, Garateguy G, Carrillo R, Arce GR (2011) Multiresolution information mining for pavement crack image analysis. *J Comput Civ Eng* 26(6):741–749
- Adu-Gyamfi YO, Kambhamettu C, Okine NA (2013) Performance assessment of flexible pavements using active contour models. In: 2013 Airfield and highway pavement conference: sustainable and efficient pavements. Los Angeles
- Adu-Gyamfi YO, Tienaa T, Attoh-Okine NO, Kambhamettu C (2014) Functional evaluation of pavement condition using a complete vision system. *J Transp Eng* 140(9):04014040
- Aghaeyan A, Abdollahi F, Talebi HA (2015) UAV–UGVs cooperation: with a moving center based trajectory. *Robot Auton Syst* 63(Part 1):1–9
- Ahmed M, Haas CT, Haas R (2011) Toward low-cost 3D automatic pavement distress surveying: the close range photogrammetry approach. *Can J Civ Eng* 38(12):1301–1313
- Amhaz R, Chambon S, Idier J, Baltazart V (2014) A new minimal path selection algorithm for automatic crack detection on pavement images. In: 2014 IEEE international conference on image processing, ICIP 2014. Institute of Electrical and Electronics Engineers Inc
- Ang JC, Haron H, Hamed HNA (2015) Semi-supervised SVM-based feature selection for cancer classification using microarray gene expression data. Current approaches in applied artificial intelligence. Springer, New York, pp 468–477
- Asensio-Cubero J, Gan JQ, Palaniappan R (2016) Multiresolution analysis over graphs for a motor imagery based online BCI game. *Comput Biol Med* 68:21–26
- Atkinson J, Campos D (2016) Improving BCI-based emotion recognition by combining EEG feature selection and kernel classifiers. *Exp Syst Appl* 47:35–41
- Attoh-Okine N, Barner K, Bentil D, Zhang R (2008) The empirical mode decomposition and the Hilbert-Huang transform. *EURASIP J Adv Signal Process* 2008(1):1–2
- Avdiyenko L, Bertschinger N, Jost J (2015) Adaptive information-theoretical feature selection for pattern classification. *Computational intelligence*. Springer, New York, pp 279–294
- Avila M, Begot S, Duculty F, Nguyen TS (2014) 2D image based road pavement crack detection by calculating minimal paths and dynamic programming. In: 2014 IEEE international conference on image processing, ICIP 2014
- Ayenu-Prah A, Attoh-Okine N (2008) Evaluating pavement cracks with bidimensional empirical mode decomposition. *EURASIP J Adv Signal Process* 2008(1):861701
- Basavaprasad B, Ravi M (2014) A comparative study on classification of image segmentation methods with a focus on graph based techniques. *Int J Res Eng Technol* 3(03):310–314
- Battiti R (1994) Using mutual information for selecting features in supervised neural net learning. *IEEE Trans Neural Netw* 5(4):537–550
- Bayındır L (2016) A review of swarm robotics tasks. *Neurocomputing* 172:292–321
- Bermejo P, Gámez JA, Puerta JM (2011) A GRASP algorithm for fast hybrid (filter-wrapper) feature subset selection in high-dimensional datasets. *Pattern Recognit Lett* 32(5):701–711
- Bhardwaj A, Sam L, Akanksha F, Martín-Torres J, Kumar R (2016) UAVs as remote sensing platform in glaciology: present applications and future prospects. *Remote Sens Environ* 175:196–204
- Bianchini A, Bandini P (2010) Prediction of pavement performance through neuro-fuzzy reasoning. *Comput Aided Civ Infrastruct Eng* 25(1):39–54
- Bray J, Verma B, Li X, He W (2006) A neural network based technique for automatic classification of road cracks. In: International joint conference on neural networks, 2006. IJCNN'06. IEEE
- Burattini E, De Gregorio M, Rossi S (2010) An adaptive oscillatory neural architecture for controlling behavior based robotic systems. *Neurocomputing* 73(16–18):2829–2836
- Bursanescu L, Blais F (1997) Automated pavement distress data collection and analysis: a 3-D approach
- Cadenas J, Garrido M, Martínez R (2015) Selecting features from low quality datasets by a fuzzy ensemble. *Computational intelligence*. Springer, New York, pp 229–243
- Cai D, Zhang C, He X (2010) Unsupervised feature selection for multi-cluster data. In: Proceedings of the 16th ACM SIGKDD international conference on knowledge discovery and data mining. ACM
- Cai Y, Zhang Y (2011) Research on pavement crack recognition methods based on image processing. In: 3rd International conference on digital image processing, ICDIP 2011. Chengdu
- Canny J (1986) A computational approach to edge detection. *IEEE Trans Pattern Anal Mach Intell* 6:679–698
- Ceylan H, Bayrak MB, Gopalakrishnan K (2014) Neural networks applications in pavement engineering: a recent survey. *Int J Pavement Res Technol* 7(6):434–444
- Chambon S, Gourraud C, Moliard JM, Nicolle P (2010) Road crack extraction with adapted filtering and Markov model-based segmentation: introduction and validation. In: 5th International conference on computer vision theory and applications, VISAPP 2010. Angers
- Chambon S, Moliard J (2011) Automatic road pavement assessment with image processing: review and comparison. *Int J Geophys* 2011:20
- Chandrashekar G, Sahin F (2014) A survey on feature selection methods. *Comput Electr Eng* 40(1):16–28
- Chang-ping W (2008) Bayes discriminant analysis method of rock-mass quality classification. *J China Coal Soc* 33(4):395–399
- Changxia M, Wenming W, Chunxia Z, Feng D, Zhengli Z (2009) Pavement cracks detection based on FDWT. In: International conference on computational intelligence and software engineering, 2009. CiSE 2009
- Chapeleau X, Blanc J, Hornych P, Gautier JL, Carroget J (2014) Use of distributed fiber optic sensors to detect damage in a pavement. In: Asphalt pavements: proceedings of the international conference on asphalt pavements, ISAP 2014
- Chen Y-C, Yang C-E, Kang S-C (2014) A lightweight bridge inspection system using a dual-cable suspension mechanism. *Autom Constr* 46:52–63
- Cheng H-D (1996) Automated real-time pavement distress detection using fuzzy logic and neural network. In: Nondestructive evaluation techniques for aging infrastructure and manufacturing. International Society for Optics and Photonics
- Cheng H-D, Chen J-R, Glazier C (1996) Novel fuzzy logic approach to pavement distress detection. In: Nondestructive evaluation techniques for aging infrastructure and manufacturing. International Society for Optics and Photonics
- Cheng H, Chen J-R, Glazier C, Hu Y (1999) Novel approach to pavement cracking detection based on fuzzy set theory. *J Comput Civ Eng* 13(4):270–280
- Cheng H, Wang J, Hu Y, Glazier C, Shi X, Chen X (2001) Novel approach to pavement cracking detection based on neural network. *Trans Res Rec J Transp Res Board* 1764:119–127

40. Chotiprayanakul P, Liu DK, Dissanayake G (2012) Human–robot–environment interaction interface for robotic grit-blasting of complex steel bridges. *Autom Constr* 27:11–23
41. Chou J, O'Neill WA, Cheng H (1994) Pavement distress classification using neural networks. In: IEEE international conference on systems, man, and cybernetics, 1994. Humans, information and technology, 1994. IEEE
42. Chou J, O'Neill WA, Cheng H (1995) Pavement distress evaluation using fuzzy logic and moment invariants. *Transp Res Rec* 1505:39–46
43. Chua KM, Xu L (1994) Simple procedure for identifying pavement distresses from video images. *J Transp Eng* 120 (3):412–431
44. Chu B, Jung K, Lim M-T, Hong D (2013) Robot-based construction automation: an application to steel beam assembly (Part I). *Autom Constr* 32:46–61
45. Chu J-W, Chu X-M, Wang R-B, Shi S-M (2003) Research on asphalt pavement surface distress image feature extraction method. *J Image Graph* 10:1211–1217
46. Colomina I, Molina P (2014) Unmanned aerial systems for photogrammetry and remote sensing: a review. *ISPRS J Photogramm Remote Sens* 92:79–97
47. Cong F, Hautakangas H, Nieminen J, Mazhelis O, Perttunen M, Riekkilä J, Ristaniemi T (2013) Applying wavelet packet decomposition and one-class support vector machine on vehicle acceleration traces for road anomaly detection. *Advances in neural networks–ISNN 2013*. Springer, New York, pp 291–299
48. Cord A, Chambon S (2012) Automatic road defect detection by textural pattern recognition based on AdaBoost. *Comput Aided Civ Infrastruct Eng* 27(4):244–259
49. Doquire G, Verleysen M (2013) Mutual information-based feature selection for multilabel classification. *Neurocomputing* 122:148–155
50. Duerden T (2004) An aura of confusion Part 2: the aided eye —‘imaging the aura?’. *Complement Ther Nurs Midwifery* 10 (2):116–123
51. Duerden T (2004) An aura of confusion: ‘seeing auras—vital energy or human physiology?’ Part 1 of a three part series. *Complement Ther Nurs Midwifery* 10(1):22–29
52. Dy JG (2008) Unsupervised feature selection. *Comput Methods Feature Sel* 19–39
53. Dy JG, Brodley CE (2004) Feature selection for unsupervised learning. *J Mach Learn Res* 5:845–889
54. ElAlami ME (2009) A filter model for feature subset selection based on genetic algorithm. *Knowl Based Syst* 22(5):356–362
55. Fawcett T (2006) An introduction to ROC analysis. *Pattern Recognit Lett* 27(8):861–874
56. Ferguson RA, Pratt DN, Turtle PR, MacIntyre IB, Moore DP, Kearney PD, Best MJ, Gardner JL, Berman M, Buckley MJ (2003) Road pavement deterioration inspection system. Google Patents
57. Fernandez-Leon JA, Acosta GG, Rozenfeld A (2014) How simple autonomous decisions evolve into robust behaviours? A review from neurorobotics, cognitive, self-organized and artificial immune systems fields. *Biosystems* 124:7–20
58. Files BT, Marathe AR (2016) A regression method for estimating performance in a rapid serial visual presentation target detection task. *J Neurosci Methods* 258:114–123
59. Foithong S, Pinnern O, Attachoo B (2012) Feature subset selection wrapper based on mutual information and rough sets. *Exp Syst Appl* 39(1):574–584
60. Gao X, Deng X, Chen N, Luo W, Hu L, Jackson T, Chen H (2011) Attentional biases among body-dissatisfied young women: an ERP study with rapid serial visual presentation. *Int J Psychophysiol* 82(2):133–142
61. Gavilán M, Balcones D, Marcos O, Llorca DF, Sotelo MA, Parra I, Ocaña M, Aliseda P, Yarla P, Amírola A (2011) Adaptive road crack detection system by pavement classification. *Sensors* 11(10):9628–9657
62. Gerson AD, Parra LC, Sajda P (2006) Cortically coupled computer vision for rapid image search. *IEEE Trans Neural Syst Rehabil Eng* 14(2):174–179
63. Golparvar-Fard M, Balali V, De La Garza JM (2015) Segmentation and recognition of highway assets using image-based 3D point clouds and semantic Texton Forests. *J Comput Civ Eng* 29 (1):04014023
64. Grandsaert PJ (2015) Integrating pavement crack detection and analysis using autonomous unmanned aerial vehicle imagery. DTIC Document
65. Graves SW (2013) Electro-optical sensor evaluation of airfield pavement. In: Airfield and highway pavement 2013: sustainable and efficient pavements—proceedings of the 2013 airfield and highway pavement conference
66. Guan H, Li J, Yu Y, Chapman M, Wang C (2015) Automated road information extraction from mobile laser scanning data. *IEEE Trans Intell Transp Syst* 16(1):194–205
67. Guan H, Li J, Yu Y, Chapman M, Wang H, Wang C, Zhai R (2014) Iterative tensor voting for pavement crack extraction using mobile laser scanning data. *IEEE Trans Geosci Remote Sens* 53(3):1527–1537
68. Guenard A, Ciarletta L (2012) The AETOURNOS project: using a flock of UAVs as a cyber physical system and platform for application-driven research. *Proced Comput Sci* 10:939–945
69. Guo W, Soibelman L, Garrett JH Jr (2009) Automated defect detection for sewer pipeline inspection and condition assessment. *Autom Constr* 18(5):587–596
70. Haas RCG, Hudson WR, Falls LC (2015) Pavement asset management. Wiley, Hoboken
71. Hall MA (1999) Correlation-based feature selection for machine learning. The University of Waikato, Hamilton
72. Han J, Sun Z, Hao H (2015) Selecting feature subset with sparsity and low redundancy for unsupervised learning. *Knowl Based Syst* 86:210–223
73. Han Y, Yang Y, Yan Y, Ma Z, Sebe N, Zhou X (2015) Semisupervised feature selection via spline regression for video semantic recognition. *IEEE Trans Neural Netw Learn Syst* 26 (2):252–264
74. Hsu H-H, Hsieh C-W, Lu M-D (2011) Hybrid feature selection by combining filters and wrappers. *Exp Syst Appl* 38(7):8144–8150
75. Huang J-J, Cai Y-Z, Xu X-M (2008) A parameterless feature ranking algorithm based on MI. *Neurocomputing* 71(7–9):1656–1668
76. Huang J, Cai Y, Xu X (2007) A hybrid genetic algorithm for feature selection wrapper based on mutual information. *Pattern Recognit Lett* 28(13):1825–1844
77. Huang J, Liu W, Sun X (2014) A pavement crack detection method combining 2D with 3D information based on Dempster-Shafer theory. *Comput Aided Civ Infrastruct Eng* 29(4):299–313
78. Huang W, Zhang N (2012) A novel road crack detection and identification method using digital image processing techniques. In: 2012 7th International conference on computing and convergence technology (ICCT, ICEI and ICACT), ICCCT 2012. Seoul
79. Huang Y, Tsai YJ (2011) Dynamic programming and connected component analysis for an enhanced pavement distress segmentation algorithm. *Transp Res Rec* 2225:89–98
80. Huang Y, Xu B (2006) Automatic inspection of pavement cracking distress. *J Electron Imaging* 15(1):013017–013017-013016

- 81 Hubacher J (2015) The phantom leaf effect: a replication, Part 1. *J Altern Complement Med* 21(2):83–90
- 82 Huili Z, Guofeng Q, Xingjian W (2010) Improvement of canny algorithm based on pavement edge detection. In: 3rd International congress on image and signal processing (CISP), 2010
- 83 Iacoviello D, Petracca A, Spezialetti M, Placidi G (2015) A real-time classification algorithm for EEG-based BCI driven by self-induced emotions. *Comput Methods Progr Biomed* 122(3):293–303
- 84 Immerzeel WW, Kraaijenbrink PDA, Shea JM, Shrestha AB, Pellicciotti F, Bierkens MFP, de Jong SM (2014) High-resolution monitoring of Himalayan glacier dynamics using unmanned aerial vehicles. *Remote Sens Environ* 150:93–103
- 85 Jahanshahi MR, Jazizadeh F, Masri SF, Becerik-Gerber B (2012) Unsupervised approach for autonomous pavement-defect detection and quantification using an inexpensive depth sensor. *J Comput Civ Eng* 27(6):743–754
- 86 Jahanshahi MR, Karimi FJ, Masri SF, Becerik-Gerber B (2013) Autonomous pavement condition assessment. Google Patents
- 87 Jahanshahi MR, Kelly JS, Masri SF, Sukhatme GS (2009) A survey and evaluation of promising approaches for automatic image-based defect detection of bridge structures. *Struct Infrastruct Eng* 5(6):455–486
- 88 Jahanshahi MR, Masri SF (2011) A novel crack detection approach for condition assessment of structures. In: ASCE international workshop on computing in civil engineering. Miami
- 89 Jahanshahi MR, Masri SF (2012) Adaptive vision-based crack detection using 3D scene reconstruction for condition assessment of structures. *Autom Constr* 22:567–576
- 90 Jahanshahi MR, Masri SF (2013) A new methodology for non-contact accurate crack width measurement through photogrammetry for automated structural safety evaluation. *Smart Mater Struct* 22(3):035019
- 91 Jahanshahi MR, Masri SF, Padgett CW, Sukhatme GS (2013) An innovative methodology for detection and quantification of cracks through incorporation of depth perception. *Mach Vis Appl* 24(2):227–241
- 92 Jain AK (1989) Fundamentals of digital image processing. Prentice-Hall, Inc., Upper Saddle River
- 93 Jiang J, Liu H, Ye H, Feng F (2015) Crack enhancement algorithm based on improved EM. *J Inf Comput Sci* 12(3):1037–1043
- 94 Jie F, Licheng J, Fang L, Tao S, Xiangrong Z (2015) Mutual-information-based semi-supervised hyperspectral band selection with high discrimination, high information, and low redundancy. *IEEE Trans Geosci Remote Sens* 53(5):2956–2969
- 95 Jiexian Z, Lili Z, Xiang F (2012) An improved beamlet tree-structured algorithm and its application in pavement crack detection. *Sci Res Essays* 7(10):1175–1184
- 96 Jiménez-González A, Martínez-de Dios JR, Ollero A (2013) Testbeds for ubiquitous robotics: a survey. *Robot Auton Syst* 61(12):1487–1501
- 97 Jin C, Liu J, Guo J (2015) A hybrid model based on mutual information and support vector machine for automatic image annotation. *Artificial intelligence perspectives and applications*. Springer, New York, pp 29–38
- 98 Jin X, Davis CH (2005) An integrated system for automatic road mapping from high-resolution multi-spectral satellite imagery by information fusion. *Inf Fus* 6(4):257–273
- 99 Jing L, Aiqin Z (2010) Pavement crack distress detection based on image analysis. In: 2010 International conference on machine vision and human-machine interface, MVHI 2010
- 100 Jung K, Chu B, Hong D (2013) Robot-based construction automation: an application to steel beam assembly (Part II). *Autom Constr* 32:62–79
- 101 Kaseko MS, Lo Z-P, Ritchie SG (1994) Comparison of traditional and neural classifiers for pavement-crack detection. *J Transp Eng* 120(4):552–569
- 102 Kaseko MS, Ritchie SG (1993) A neural network-based methodology for pavement crack detection and classification. *Transp Res C Emerg Technol* 1(4):275–291
- 103 Kaul V, Tsai Y, Mersereau RM (2010) Quantitative performance evaluation algorithms for pavement distress segmentation. *Transp Res Rec* 2153:106–113
- 104 Kaul V, Tsai Y, Yezzi A (2010) Detection of curves with unknown endpoints using minimal path techniques. In: 2010 21st British machine vision conference, BMVC 2010, Aberystwyth, British Machine Vision Association, BMVA
- 105 Kaul V, Yezzi A, Tsai YJ (2012) Detecting curves with unknown endpoints and arbitrary topology using minimal paths. *IEEE Trans Pattern Anal Mach Intell* 34(10):1952–1965
- 106 Khan AM, Ravi S (2013) Image segmentation methods: a comparative study. *Int J Soft Comput Eng (IJSCE)* 3(4):84–92
- 107 Khoshgoftaar TM, Gao K, Napolitano A, Wald R (2014) A comparative study of iterative and non-iterative feature selection techniques for software defect prediction. *Inf Syst Front* 16(5):801–822
- 108 Kim BH, Kim M, Jo S (2014) Quadcopter flight control using a low-cost hybrid interface with EEG-based classification and eye tracking. *Comput Biol Med* 51:82–92
- 109 Kim JJ, Lee HD, Yun DG, Sung JG (2007) Development of laser pavement image processing system to enhance existing automated pavement distress detection process. In: Maintenance and rehabilitation of pavements and technological control: proceedings of the 5th international conference, MAIREPAV 2007
- 110 Kim Y-S, Haas CT, Greer R (1998) Man-machine balanced crack sealing process for UT automated road maintenance machine. In: Proceedings of the international conference on applications of advanced technologies in transportation engineering
- 111 Kim YS, Haas CT (2002) A man-machine balanced rapid object model for automation of pavement crack sealing and maintenance. *Can J Civ Eng* 29(3):459–474
- 112 Kim YS, Haas CT, Greer R (1998) Path planning for machine vision assisted, teleoperated pavement crack sealer. *J Transp Eng* 124(2):137–143
- 113 Koch C, Brilakis I (2011) Automated detection of potholes in visual data. In: ISEC 2011: 6th international structural engineering and construction conference—modern methods and advances in structural engineering and construction
- 114 Koch C, Georgieva K, Kasireddy V, Akinci B, Fieguth P (2015) A review on computer vision based defect detection and condition assessment of concrete and asphalt civil infrastructure. *Adv Eng Inform* 29(2):196–210
- 115 Kostavelis I, Gasteratos A (2015) Semantic mapping for mobile robotics tasks: a survey. *Robot Auton Syst* 66:86–103
- 116 Koutsopoulos H, Downey A (1993) Primitive-based classification of pavement cracking images. *J Transp Eng* 119(3):402–418
- 117 Koutsopoulos HN, El Sanhoury I, Downey AB (1993) Analysis of segmentation algorithms for pavement distress images. *J Transp Eng* 119(6):868–888
- 118 Kruglova T, Sayfeddine D, Vitaliy K (2015) Robotic laser inspection of airplane wings using quadrotor. *Procedia Eng* 129:245–251
- 119 Kumar V, Chhabra JK, Kumar D (2015) Automatic unsupervised feature selection using gravitational search algorithm. *IETE J Res* 61(1):22–31
- 120 Kupferberg A, Glasauer S, Burkart JM (2013) Do robots have goals? How agent cues influence action understanding in non-human primates. *Behav Brain Res* 246:47–54

- 121 Laurent J, Doucet M (2010) Vision system and a method for scanning a traveling surface to detect surface defects thereof. Google Patents
- 122 LeBlanc J, Gennert MA, Wittels N, Gosselin D (1991) Analysis and generation of pavement distress images using fractals. *Transp Res Rec* (1311)
- 123 Lee BJ, Lee H (2004) Position-invariant neural network for digital pavement crack analysis. *Comput Aided Civ Infrastruct Eng* 19(2):105–118
- 124 Lee J, Kim D-W (2015) Mutual information-based multi-label feature selection using interaction information. *Exp Syst Appl* 42(4):2013–2025
- 125 Leong BTM, Low SM, Ooi MP-L (2012) Low-cost microcontroller-based hover control design of a quadcopter. *Procedia Eng* 41:458–464
- 126 Lettsome CA, Tsai Y (2012) An automated filter bank-based pavement crack detection system incorporating standard compression coders. *Int J Pavement Res Technol* 5(3):176–186
- 127 Li G (2012) Improved pavement distress detection based on contourlet transform and multi-direction morphological structuring elements. *Appl Mech Mater* 466–467:371–375
- 128 Li G (2012) Improved pavement distress detection based on contourlet transform and multi-direction morphological structuring elements. In: 2012 International conference on intelligent system and applied material, GSAM 2012, vol 466. Taiyuan, pp 371–375
- 129 Li G (2013) New weighted mean filtering algorithm for surface image based on grey entropy. *Sens Transducers* 161(12):21–26
- 130 Li G, Xu Y, Li J (2013) Fuzzy contrast enhancement algorithm for road surface image based on adaptively changing index via grey entropy. *Inf Technol J* 12(19):5309–5314
- 131 Li L, Sun LJ, Tan SG, Ning GB (2012) An efficient way in image preprocessing for pavement crack images. In: CICTP 2012: multimodal transportation systems—convenient, safe, cost-effective, efficient—proceedings of the 12th COTA international conference of transportation professionals
- 132 Li L, Sun LJ, Tan SG, Ning GB (2012) An efficient way in image preprocessing for pavement crack images. In: 12th COTA international conference of transportation professionals: multimodal transportation systems—convenient, safe, cost-effective, efficient, CICTP 2012. Beijing
- 133 Li M, Stein A, Bijker W, Zhan Q (2016) Region-based urban road extraction from VHR satellite images using binary partition tree. *Int J Appl Earth Obs Geoinform* 44:217–225
- 134 Li N, Hou X, Yang X, Dong Y (2009) Automation recognition of pavement surface distress based on support vector machine. In: Second international conference on intelligent networks and intelligent systems, 2009. ICINIS'09. IEEE
- 135 Li Q, Zou Q, Zhang D, Mao Q (2011) FoSA: F* seed-growing approach for crack-line detection from pavement images. *Image Vis Comput* 29(12):861–872
- 136 Lin J, Liu Y (2010) Potholes detection based on SVM in the pavement distress image. In: Ninth international symposium on distributed computing and applications to business engineering and science (DCABES), 2010 IEEE
- 137 Ling L, Peikang H, Xiaohu W, Xudong P (2009) Image edge detection based on beamlet transform. *J Syst Eng Electron* 20(1):1–5
- 138 Liu F, Xu G, Yang Y, Niu X, Pan Y (2008) Novel approach to pavement cracking automatic detection based on segment extending. In: International symposium on knowledge acquisition and modeling, 2008. KAM'08. IEEE
- 139 Liu H, Sun J, Liu L, Zhang H (2009) Feature selection with dynamic mutual information. *Pattern Recognit* 42(7):1330–1339
- 140 Lokeshwor H, Das LK, Goel S (2013) Robust method for automated segmentation of frames with/without distress from road surface video clips. *J Transp Eng* 140(1):31–41
- 141 Lokeshwor H, Das LK, Goel S (2014) Robust method for automated segmentation of frames with/without distress from road surface video clips. *J Transp Eng* 140(1):31–41
- 142 Luo W, Feng W, He W, Wang N-Y, Luo Y-J (2010) Three stages of facial expression processing: ERP study with rapid serial visual presentation. *NeuroImage* 49(2):1857–1867
- 143 Ma C-X, Zhao C-X, Hou Y-K (2008) Pavement distress detection based on nonsampled contourlet transform. In: International conference on computer science and software engineering, 2008, IEEE
- 144 Mahler DS, Kharoufa ZB, Wong EK, Shaw LG (1991) Pavement distress analysis using image processing techniques. *Comput Aided Civ Infrastruct Eng* 6(1):1–14
- 145 Maini R, Aggarwal H (2009) Study and comparison of various image edge detection techniques. *Int J Image Process (IJIP)* 3(1):1–11
- 146 Maldonado S, Carrizosa E, Weber R (2015) Kernel Penalized K-means: a feature selection method based on Kernel K-means. *Inf Sci* 322:150–160
- 147 Mancini A, Malinverni ES, Frontoni E, Zingaretti P (2013) Road pavement crack automatic detection by MMS images. In: 2013 21st Mediterranean conference on control and automation, MED 2013—conference proceedings
- 148 Marques AGCS, Correia PL (2012) Automatic road pavement crack detection using SVM. Lisbon, Portugal: Dissertation for the Master of Science Degree in Electrical and Computer Engineering at Instituto Superior Técnico
- 149 Mathavan S, Kamal K, Rahman M (2015) A review of three-dimensional imaging technologies for pavement distress detection and measurements. *IEEE Trans Intell Transp Syst* 16(5):2353–2362
- 150 McCane LM, Heckman SM, McFarland DJ, Townsend G, Mak JN, Sellers EW, Zeitlin D, Tenteromano LM, Wolpaw JR, Vaughan TM (2015) P300-based brain-computer interface (BCI) event-related potentials (ERPs): people with amyotrophic lateral sclerosis (ALS) vs. age-matched controls. *Clin Neurophysiol* 126(11):2124–2131
- 151 McCune RR, Madey GR (2014) Control of Artificial Swarms with DDDAS. *Procedia Comput Sci* 29:1171–1181
- 152 McGhee KH (2004) Automated pavement distress collection techniques. *Transp Res Board* 334
- 153 McNeil S, Humplick F (1991) Evaluation of errors in automated pavement-distress data acquisition. *J Transp Eng* 117(2):224–241
- 154 Mertz C, Varadharajan S, Jose S, Sharma K, Wander L, Wang J (2014) City-wide road distress monitoring with smartphones. In: 21st World congress on intelligent transport systems: reinventing transportation in our connected world, ITSWC 2014, intelligent transport systems (ITS)
- 155 Metni N, Hamel T (2007) A UAV for bridge inspection: visual servoing control law with orientation limits. *Autom Constr* 17(1):3–10
- 156 Michaelsen E, Meidow J (2014) Stochastic reasoning for structural pattern recognition: an example from image-based UAV navigation. *Pattern Recognit* 47(8):2732–2744
- 157 Mitra P, Murthy C, Pal SK (2002) Unsupervised feature selection using feature similarity. *IEEE Trans Pattern Anal Mach Intell* 24(3):301–312
- 158 Moazzam I, Kamal K, Mathavan S, Usman S, Rahman M (2013) Metrology and visualization of potholes using the microsoft kinect sensor. In: IEEE conference on intelligent transportation systems, proceedings, ITSC
- 159 Nejad FM, Zakeri H (2011) A comparison of multi-resolution methods for detection and isolation of pavement distress. *Exp Syst Appl* 38(3):2857–2872
- 160 Mohajeri MJH, Manning PJ (1991) Aria (trademark): an operating system of pavement distress diagnosis by image processing. *Transp Res Rec* 1311

- 161 Mokhtari S (2015) Analytical study of computer vision-based pavement crack quantification using machine learning techniques. University of Central Florida Orlando, Florida
- 162 Montero R, Victores JG, Martínez S, Jardón A, Balaguer C (2015) Past, present and future of robotic tunnel inspection. *Autom Constr* 59:99–112
- 163 Moussa G, Hussain K (2011) A new technique for automatic detection and parameters estimation of pavement crack. In: 4th International multi-conference on engineering and technological innovation, IMETI 2011. Orlando
- 164 Na W, Tao W (2012) Proximal support vector machine based pavement image classification. In: 2012 IEEE 5th international conference on advanced computational intelligence, ICACI 2012. Nanjing
- 165 Naidoo T, Joubert D, Chiwewe T, Tyatyantsi A, Rancati B, Mbizeni A (2014) Visual surveying platform for the automated detection of road surface distresses. In: Proceedings of SPIE: the international society for optical engineering
- 166 Natalizio E, Di Caro G, Sekercioglu A, Yanmaz E (2013) A special issue of Ad Hoc Networks on “Theory, algorithms and applications of wireless networked robotics”. *Ad Hoc Netw* 11(7):1891–1892
- 167 Nejad FM, Zakeri H (2011) An expert system based on wavelet transform and radon neural network for pavement distress classification. *Exp Syst Appl* 38(6):7088–7101
- 168 Nejad FM, Zakeri H (2011) An optimum feature extraction method based on Wavelet–Radon transform and dynamic neural network for pavement distress classification. *Exp Syst Appl* 38(8):9442–9460
- 169 Nejad FM, Zakeri H (2012) The hybrid method and its application to smart pavement management. *Metaheuristics Water Geotech Transp Eng* 439
- 170 Nguyen T, Khosravi A, Creighton D, Nahavandi S (2015) EEG signal classification for BCI applications by wavelets and interval type-2 fuzzy logic systems. *Exp Syst Appl* 42(9):4370–4380
- 171 Nguyen TS, Avila M, Begot S (2009) Automatic detection and classification of defect on road pavement using anisotropy measure. In: Signal processing conference, 2009 17th European. IEEE, pp 617–621
- 172 Ni Z, Tang P, Xi Y (2012) A new method to pavement cracking detection based on the biological inspired model. In: 2012 International conference on computer science and information processing, CSIP 2012. Xi’an
- 173 Nishikawa T, Yoshida J, Sugiyama T, Fujino Y (2012) Concrete crack detection by multiple sequential image filtering. *Comput Aided Civ Infrastruct Eng* 27(1):29–47
- 174 Oh J-K, Jang G, Oh S, Lee JH, Yi B-J, Moon YS, Lee JS, Choi Y (2009) Bridge inspection robot system with machine vision. *Autom Constr* 18(7):929–941
- 175 Oliveira H, Caeiro J, Correia PL (2014) Accelerated unsupervised filtering for the smoothing of road pavement surface imagery. In: European signal processing conference
- 176 Oliveira H, Caeiro JJ, Correia PL (2010) Improved road crack detection based on one-class Parzen density estimation and entropy reduction. In: 2010 17th IEEE international conference on image processing, ICIP 2010. Hong Kong
- 177 Oliveira H, Correia PL (2008) Supervised strategies for cracks detection in images of road pavement flexible surfaces. In: Signal processing conference, 2008 16th European, IEEE
- 178 Oliveira H, Correia PL (2010) Automatic crack detection on road imagery using anisotropic diffusion and region linkage. In: 18th European signal processing conference, EUSIPCO 2010. Aalborg
- 179 Oliveira H, Correia PL (2013) Automatic road crack detection and characterization. *IEEE Trans Intell Transp Syst* 14(1):155–168
- 180 Oliveira H, Correia PL (2014) CrackIT: an image processing toolbox for crack detection and characterization. In: 2014 IEEE international conference on image processing, ICIP 2014
- 181 Ouyang A, Dong Q, Wang Y, Liu Y (2014) The classification of pavement crack image based on beamlet algorithm. In: 7th IFIP WG 5.14 international conference on computer and computing technologies in agriculture, CCTA 2013
- 182 Ouyang A, Wang Y (2012) Edge detection in pavement crack image with beamlet transform. In: 2012 2nd International conference on electronic and mechanical engineering and information technology, EMEIT 2012. Shenyang
- 183 Ouyang W, Xu B (2013) Pavement cracking measurements using 3D laser-scan images. *Meas Sci Technol* 24(10):105204
- 184 Paraforos DS, Griepentrog HW, Vougioukas SG (2016) Country road and field surface profiles acquisition, modelling and synthetic realisation for evaluating fatigue life of agricultural machinery. *J Terramech* 63:1–12
- 185 Peng K, Cai G, Chen BM, Dong M, Lum KY, Lee TH (2009) Design and implementation of an autonomous flight control law for a UAV helicopter. *Automatica* 45(10):2333–2338
- 186 Prakash S, Chowdhury AR, Gupta A (2015) Monitoring the human health by measuring the biofield “aura”: an overview. *Int J Appl Eng Res* 10(2765427658)
- 187 ZPynn J, Wright A, Lodge R (1999) Automatic identification of cracks in road surfaces. In: Image processing and its applications, 1999. Seventh International Conference on (Conf. Publ. No. 465)
- 188 Qureshi B, Koubâa A (2014) Five traits of performance enhancement using cloud robotics: a survey. *Procedia Comput Sci* 37:220–227
- 189 Rababaah H (2005) Asphalt pavement crack classification: a comparative study of three ai approaches—multilayer perceptron, genetic algorithms, and self-organizing maps. Citeseer
- 190 Rababaah H, Vrajitoru D, Wolfer J (2005) Asphalt pavement crack classification: a comparison of GA, MLP, and SOM. In: Proceedings of genetic and evolutionary computation conference. Late-Breaking Paper
- 191 Radopoulou SC, Brilakis I (2015) Patch detection for pavement assessment. *Autom Constr* 53:95–104
- 192 Rai R, Deshpande AV (2016) Fragmentary shape recognition: a BCI study. *Comput Aided Des* 71:51–64
- 193 Raman M, Hossain M, Miller R, Cumberledge G, Lee H, Kang K (2004) Assessment of image-based data collection and the AASHTO provisional standard for cracking on asphalt-surfaced pavements. *Transp Res Rec J Transp Res Board* 1889:116–125
- 194 Reeves B (2011) High speed photometric stereo pavement scanner. Google Patents
- 195 Roca D, Lagüela S, Díaz-Vilariño L, Armesto J, Arias P (2013) Low-cost aerial unit for outdoor inspection of building façades. *Autom Constr* 36:128–135
- 196 Rouillard J, Duprès A, Cabestaing F, Leclercq S, Bekaert M-H, Piau C, Vannobel J-M, Lecocq C (2015) Hybrid BCI coupling EEG and EMG for severe motor disabilities. *Procedia Manuf* 3:29–36
- 197 Saar T, Talvik O (2010) Automatic asphalt pavement crack detection and classification using neural networks. In: Electronics conference (BEC), 2010 12th Biennial Baltic, IEEE
- 198 Salari E, Bao G (2010) Pavement distress detection and classification using feature mapping. In: 2010 IEEE international conference on electro/information technology, EIT2010. Normal
- 199 Salari E, Bao G (2011) Pavement distress detection and severity analysis. In: Proceedings of SPIE. The International Society for Optical Engineering
- 200 Salari E, Ouyang D (2012) An image-based pavement distress detection and classification. In: 2012 IEEE international conference on electro/information technology, EIT 2012. Indianapolis

- 201 Salari E, Yu X (2011) Pavement distress detection and classification using a Genetic Algorithm. In: Applied imagery pattern recognition workshop (AIPR), 2011 IEEE, IEEE
- 202 Salman M, Mathavan S, Kamal K, Rahman M (2013) Pavement crack detection using the Gabor filter. In: 2013 16th international IEEE conference on intelligent transportation systems: intelligent transportation systems for all modes, ITSC 2013. The Hague
- 203 Schnebele E, Tanyu BF, Cervone G, Waters N (2015) Review of remote sensing methodologies for pavement management and assessment. *Eur Transp Res Rev* 7(2):1–19
- 204 Senanayake M, Senthoooran I, Barca JC, Chung H, Kamruzzaman J, Murshed M (2016) Search and tracking algorithms for swarms of robots: a survey. *Robot Auton Syst* 75(Part B):422–434
- 205 Senthilkumaran N, Rajesh R (2009) Edge detection techniques for image segmentation—a survey of soft computing approaches. *Int J Recent Trends Eng* 1(2)
- 206 Senthilkumaran N, Rajesh R (2009) Image segmentation—a survey of soft computing approaches. In: International conference on advances in recent technologies in communication and computing, 2009. ARTCom'09. IEEE, pp 844–846
- 207 Sharifi M, Fathy M, Mahmoudi MT (2002) A classified and comparative study of edge detection algorithms. In: Proceedings international conference on information technology: coding and computing, 2002. IEEE
- 208 Shen Y, Dang JW, Wang YP, Feng X (2014) A compressed sensing pavement distress image filtering algorithm based on NSCT domain. *J Optoelectron Laser* 25(8):1620–1626
- 209 Shi C, Ruan Q, An G, Zhao R (2015) Hessian semi-supervised sparse feature selection based on-matrix norm. *IEEE Trans Multimed* 17(1):16–28
- 210 Shukla A, Karki H (2016) Application of robotics in offshore oil and gas industry: a review Part II. *Robot Auton Syst* 75(Part B):508–524
- 211 Shukla A, Karki H (2016) Application of robotics in onshore oil and gas industry: a review Part I. *Robot Auton Syst* 75(Part B):490–507
- 212 Siebert S, Teizer J (2014) Mobile 3D mapping for surveying earthwork projects using an Unmanned Aerial Vehicle (UAV) system. *Autom Constr* 41:1–14
- 213 Solla M, Lagüela S, González-Jorge H, Arias P (2014) Approach to identify cracking in asphalt pavement using GPR and infrared thermographic methods: preliminary findings. *NDT E Int* 62:55–65
- 214 Song B, Wei N (2013) Statistics properties of asphalt pavement images for cracks detection. *J Inf Comput Sci* 10(9):2833–2843
- 215 Song H, Wang W, Wang F, Wu L, Wang Z (2015) Pavement crack detection by ridge detection on fractional calculus and dual-thresholds. *Int J Multimed Ubiquitous Eng* 10(4):19–30
- 216 Sridevi M, Mala C (2012) A survey on monochrome image segmentation methods. *Procedia Technol* 6:548–555
- 217 Stamatescu V, Wong S, Kearney D, Lee I, Milton A (2015) Mutual information for enhanced feature selection in visual tracking. In: SPIE defense + security. International Society for Optics and Photonics
- 218 Su YS, Kang SC, Chang JR, Hsieh SH (2013) Dual-light inspection method for automatic pavement surveys. *J Comput Civ Eng* 27(5):534–543
- 219 Sun X, Huang J, Liu W, Xu M (2012) Pavement crack characteristic detection based on sparse representation. *EURASIP J Adv Signal Process* 2012(1):1–11
- 220 Sun ZY, Hao XL, Li W, Yuan MX (2015) Research of pavement 3D data denoising algorithm. *J Chang Univ (Nat Sci Ed)* 35(1):20–25
- 221 Sun ZY, Zhao HW, Li W, Hao XL, Huyan J (2015) 3D pavement crack identification method based on dual-phase scanning detection. *China J Highway Transp* 28(2):26–32
- 222 Sundin S, Braban-Ledoux C (2001) Artificial intelligence-based decision support technologies in pavement management. *Comput Aided Civ Infrastruct Eng* 16(2):143–157
- 223 Tan Y, Zheng Z-Y (2013) Research advance in swarm robotics. *Def Technol* 9(1):18–39
- 224 Tang J, Gu Y (2013) Automatic crack detection and segmentation using a hybrid algorithm for road distress analysis. In: 2013 IEEE international conference on systems, man, and cybernetics, SMC 2013. Manchester
- 225 Terzi S (2013) Modeling for pavement roughness using the ANFIS approach. *Adv Eng Softw* 57:59–64
- 226 Timm DH, McQueen JM (2004) A study of manual vs. automated pavement condition surveys. Auburn University, Alabama
- 227 Tomiyama K, Kawamura A, Ishida T (2013) Automatic detection method of localized pavement roughness using quarter car model by lifting wavelet filters. *Int J Pavement Res Technol* 6(5):627–632
- 228 Tong H, Chao WW, Qiang HC, Bo XY (2012) Path planning of UAV based on voronoi diagram and DPSO. *Procedia Eng* 29:4198–4203
- 229 Tsai Y-C, Kaul V, Mersereau RM (2009) Critical assessment of pavement distress segmentation methods. *J Transp Eng* 136(1):11–19
- 230 Tsai Y, Kaul V, Yezzi A (2013) Automating the crack map detection process for machine operated crack sealer. *Autom Constr* 31:10–18
- 231 Tsai YC, Jiang C, Huang Y (2014) Multiscale crack fundamental element model for real-world pavement crack classification. *J Comput Civ Eng* 28(4):04014012
- 232 Tsai YC, Kaul V, Lettsome CA (2012) Enhanced adaptive filterbank-based automated pavement crack detection and segmentation system. *J Electron Imaging* 21(4):043008-043008
- 233 Tsai YC, Kaul V, Mersereau RM (2010) Critical assessment of pavement distress segmentation methods. *J Transp Eng* 136(1):11–19
- 234 Tsai YJ, Li F (2012) Critical assessment of detecting asphalt pavement cracks under different lighting and low intensity contrast conditions using emerging 3D laser technology. *J Transp Eng* 138(5):649–656
- 235 Tseng Y-H, Kang S-C, Chang J-R, Lee C-H (2011) Strategies for autonomous robots to inspect pavement distresses. *Autom Constr* 20(8):1156–1172
- 236 Uncu Ö, Türkşen IB (2007) A novel feature selection approach: combining feature wrappers and filters. *Inf Sci* 177(2):449–466
- 237 Varadharajan S, Jose S, Sharma K, Wander L, Mertz C (2014) Vision for road inspection. In: IEEE winter conference on applications of computer vision (WACV), 2014 IEEE
- 238 Varela G, Caamaño P, Orjales F, Deibe Á, López-Peña F, Duro RJ (2014) Autonomous UAV based search operations using constrained sampling evolutionary algorithms. *Neurocomputing* 132:54–67
- 239 Vasuki Y, Holden E-J, Kovesi P, Micklethwaite S (2014) Semi-automatic mapping of geological Structures using UAV-based photogrammetric data: an image analysis approach. *Comput Geosci* 69:22–32
- 240 Velinsky SA, Feng X, Bennett DA (2003) Operator controlled, vehicle-based highway crack-sealing machine. *Heavy Veh Syst* 10(3):145–166
- 241 Verma SK, Chauhan R (2014) Nanorobotics in dentistry: a review. *Indian J Dent* 5(Supplement):62–70

- 242 Victores JG, Martínez S, Jardón A, Balaguer C (2011) Robot-aided tunnel inspection and maintenance system by vision and proximity sensor integration. *Autom Constr* 20(5):629–636
- 243 Wang C, Sha A, Sun Z (2010) Pavement crack classification based on chain code. In: Seventh international conference on fuzzy systems and knowledge discovery (FSKD), 2010, IEEE
- 244 Wang J, Gao RX (2012) Pavement distress analysis based on dual-tree complex wavelet transform. *Int J Pavement Res Technol* 5(5):283–288
- 245 Wang JJ-Y, Huang JZ, Sun Y, Gao X (2015) Feature selection and multi-kernel learning for adaptive graph regularized non-negative matrix factorization. *Exp Syst Appl* 42(3):1278–1286
- 246 Wang K (2000) Designs and implementations of automated systems for pavement surface distress survey. *J Infrastruct Syst* 6(1):24–32
- 247 Wang K, Li Q, Gong W (2008) Wavelet-based pavement distress image edge detection with a trous algorithm. *Transp Res Rec J Transp Res Board* 2024:73–81
- 248 Wang KCP, Li Q, Gong W (2007) Wavelet-based pavement distress image edge detection with a trous algorithm. *Transp Res Rec* 2024:73–81
- 249 Wang S, Pedrycz W, Zhu Q, Zhu W (2015) Unsupervised feature selection via maximum projection and minimum redundancy. *Knowl Based Syst* 75:19–29
- 250 Wang S, Tang W (2011) Pavement crack segmentation algorithm based on local optimal threshold of cracks density distribution. In: 7th International conference on intelligent computing, ICIC 2011. Zhengzhou. 6838 LNCS, pp 298–302
- 251 Wang S, Tang W (2011) Pavement crack segmentation algorithm based on local optimal threshold of cracks density distribution. In: Lecture notes in computer science (including subseries lecture notes in artificial intelligence and lecture notes in bioinformatics). 6838 LNCS, pp 298–302
- 252 Wang X, Feng X (2011) Pavement distress detection and classification with automated image processing. In: Proceedings 2011 international conference on transportation, mechanical, and electrical engineering, TMEE 2011
- 253 Wang Z (2000) Formulation and assessment of a customizable procedure for pavement distress index
- 254 Wang Z, Li M, Li J (2015) A multi-objective evolutionary algorithm for feature selection based on mutual information with a new redundancy measure. *Inf Sci* 307:73–88
- 255 Wei H, Li N, Liu M, Tan J (2013) A novel autonomous self-assembly distributed swarm flying robot. *Chin J Aeronaut* 26(3):791–800
- 256 Wei N, Zhao X, Dou X, Song H, Wang T (2010) Beamlet transform based pavement image crack detection. In: International conference on intelligent computation technology and automation (ICICTA), 2010, IEEE
- 257 Wirkner J, Löw A, Hamm AO, Weymar M (2015) New learning following reactivation in the human brain: targeting emotional memories through rapid serial visual presentation. *Neurobiol Learn Memory* 119:63–68
- 258 Wu C, Lu B, Chen D, Wang L (2011) Pavement image denoising based on shearlet transform. In: International conference on electronics and optoelectronics (ICEOE), 2011, IEEE
- 259 Wu S, Liu Y (2012) A segment algorithm for crack detection. In: 2012 IEEE symposium on electrical and electronics engineering, EESYM 2012. Kuala Lumpur
- 260 Xiao W-X, Zhang X, Huang W (2004) Preliminary study of pavement surface distress automation recognition based on wavelet neural network. *Shanghai Highw* 2:008
- 261 Xu G, Ma J, Liu F, Niu X (2008) Automatic recognition of pavement surface crack based on Bp neural network. In: International conference on computer and electrical engineering, 2008. ICCEE 2008. IEEE
- 262 Xu K, Wei N, Ma R (2013) Pavement crack image detection algorithm under nonuniform illuminance. In: 2013 IEEE 3rd international conference on information science and technology, ICIST 2013, Yangzhou, Jiangsu, IEEE Computer Society
- 263 Xu W, Tang Z, Xu D, Wu G (2015) Integrating multi-features fusion and gestalt principles for pavement crack detection. *J Comput Aided Des Comput Graph* 27(1):147–156
- 264 Xu W, Tang Z, Zhou J, Ding J (2013) Pavement crack detection based on saliency and statistical features. In: 2013 20th IEEE international conference on image processing, ICIP 2013. Melbourne
- 265 Yan WY, Shaker A, El-Ashmawy N (2015) Urban land cover classification using airborne LiDAR data: a review. *Remote Sens Environ* 158:295–310
- 266 Yao J, Mao Q, Goodison S, Mai V, Sun Y (2015) Feature selection for unsupervised learning through local learning. *Pattern Recognit Lett* 53:100–107
- 267 Yao M, Zhao Z, Yao X, Xu B (2015) Fusing complementary images for pavement cracking measurements. *Meas Sci Technol* 26(2):025005
- 268 Yao P, Wang H, Su Z (2015) UAV feasible path planning based on disturbed fluid and trajectory propagation. *Chin J Aeronaut* 28(4):1163–1177
- 269 Yassi M, Moattar MH (2014) Robust and stable feature selection by integrating ranking methods and wrapper technique in genetic data classification. *Biochem Biophys Res Commun* 446(4):850–856
- 270 Ying H, Zhu Q, Tan Z, Wei J (2013) Faulting estimation method based on vertical acceleration of cement concrete pavement. *J Harbin Inst Technol* 45(2):96–100
- 271 Ying L (2009) Beamlet transform based technique for pavement image processing and classification. The University of Toledo, Toledo
- 272 Ying L, Salari E (2010) Beamlet transform-based technique for pavement crack detection and classification. *Comput Aided Civ Infrastruct Eng* 25(8):572–580
- 273 Yoo H-S, Kim Y-S (2015) Development of a crack recognition algorithm from non-routed pavement images using artificial neural network and binary logistic regression. *KSCE J Civ Eng* 20:1–12
- 274 Youquan H, Hanxing Q, Jian W, Wei Z, Jianfang X (2011) Studying of road crack image detection method based on the mathematical morphology. In: 4th International congress on image and signal processing, CISP 2011. Shanghai
- 275 Yu S-N, Jang J-H, Han C-S (2007) Auto inspection system using a mobile robot for detecting concrete cracks in a tunnel. *Autom Constr* 16(3):255–261
- 276 Yuwono M, Guo Y, Wall J, Li J, West S, Platt G, Su SW (2015) Unsupervised feature selection using swarm intelligence and consensus clustering for automatic fault detection and diagnosis in heating ventilation and air conditioning systems. *Appl Soft Comput* 34:402–425
- 277 Zakeri H, Nejad FM, Fahimifar A, Torshizi AD, Zarandi MHF (2013) A multi-stage expert system for classification of pavement cracking. In: IFSA world congress and NAFIPS annual meeting (IFSA/NAFIPS), 2013 Joint
- 278 Zakeri H, Nejad FM, Fahimifar A, Torshizi AD, Zarandi MHF (2014) A new automatic MF generator (AMFG) for general 3D type-ii fuzzy in the polar frame. In: 2014 IEEE conference on norbert wiener in the 21st century: driving technology's future, 21CW 2014—incorporating the proceedings of the 2014 North American fuzzy information processing society conference, NAFIPS 2014, conference proceedings
- 279 Zalama E, Gómez-García-Bermejo J, Medina R, Llamas J (2014) Road crack detection using visual features extracted by gabor filters. *Comput Aided Civ Infrastruct Eng* 29(5):342–358

- 280 Zarco-Tejada PJ, González-Dugo V, Berni JAJ (2012) Fluorescence, temperature and narrow-band indices acquired from a UAV platform for water stress detection using a micro-hyperspectral imager and a thermal camera. *Remote Sens Environ* 117:322–337
- 281 Zarrinpanjeh N, Samadzadegan F, Schenk T (2013) A new ant based distributed framework for urban road map updating from high resolution satellite imagery. *Comput Geosci* 54:337–350
- 282 Zhang A, Li Q, Wang KCP, Qiu S (2013) Matched filtering algorithm for pavement cracking detection. *Transp Res Rec* 2367:30–42
- 283 Zhang C-K, Hu H (2005) Feature selection using the hybrid of ant colony optimization and mutual information for the forecaster. In: *Proceedings of 2005 international conference on machine learning and cybernetics*, 2005. IEEE
- 284 Zhang C, Elaksher A (2012) An unmanned aerial vehicle-based imaging system for 3D measurement of unpaved road surface distresses. *Comput Aided Civ Infrastruct Eng* 27(2):118–129
- 285 Zhang D-Q, Qu S-R, Li W-B, He L (2009) Image enhancement algorithm on ridgelet domain in detection of road cracks. *China J Highway Transp* 22(2):26–31
- 286 Zhang D, Qu S, He L, Shi S (2009) Automatic ridgelet image enhancement algorithm for road crack image based on fuzzy entropy and fuzzy divergence. *Opt Lasers Eng* 47(11):1216–1225
- 287 Zhang H, Fritts JE, Goldman SA (2008) Image segmentation evaluation: a survey of unsupervised methods. *Comput Vis Image Underst* 110(2):260–280
- 288 Zhang J, Sha A, Sun Z, Gao H (2009). Pavement crack automatic recognition based on wiener filtering. In: *Critical issues in transportation system planning, development, and management proceedings of the ninth international conference of chinese transportation professionals*
- 289 Zhang Y, Zhou H (2012) Automatic pavement cracks detection and classification using radon transform. *J Inf Comput Sci* 9 (17):5241–5247
- 290 Zhao J, Lu K, He X (2008) Locality sensitive semi-supervised feature selection. *Neurocomputing* 71(10):1842–1849
- 291 Zhao Z, Liu H (2007) Semi-supervised feature selection via spectral analysis. *SDM, SIAM*
- 292 Zhibiao S, Yanqing G (2013) Algorithm on contourlet domain in detection of road cracks for pavement images. *J Algorithms Comput Technol* 7(1):15–26
- 293 Zhou H, Yang S, Zhu J (2010) Illumination invariant enhancement and threshold segmentation algorithm for asphalt pavement crack image. In: *2010 6th International conference on wireless communications, networking and mobile computing, WiCOM 2010*. Chengdu
- 294 Zhou HL, Jiang YL, Wan X (2011) Evolving fuzzy neural network for highway subsurface condition evaluation using ground penetrating radar. *Adv Inf Sci Serv Sci* 3(9):176–182
- 295 Zhou J, Huang P, Chiang F-P (2005) Wavelet-based pavement distress classification. *Transp Res Rec J Transp Res Board* 1940 (1):89–98
- 296 Zhou J, Huang PS, Chiang F-P (2006) Wavelet-based pavement distress detection and evaluation. *Opt Eng* 45(2):027007-027007-027010
- 297 Zhu Z, German S, Brilakis I (2010) Detection of large-scale concrete columns for automated bridge inspection. *Autom Constr* 19(8):1047–1055
- 298 Zou Q, Cao Y, Li Q, Mao Q, Wang S (2012) CrackTree: automatic crack detection from pavement images. *Pattern Recognit Lett* 33(3):227–238
- 299 Zuo YX, Wang GQ, Zuo CC (2013) The segmentation algorithm for pavement cracking images based on the improved fuzzy clustering. In: *2013 2nd International conference on chemical, mechanical and materials engineering, CMME 2013*, vol 319. Melbourne. pp 362–366
- 300 长安大学 (2011) Pavement crack detection system based on image and detection method thereof. Google Patents